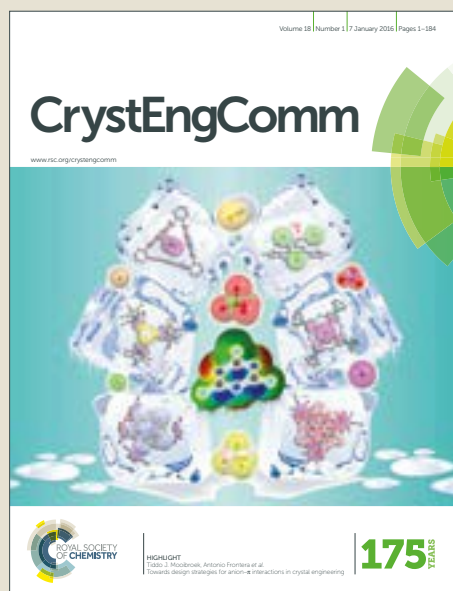


# CrystEngComm

Accepted Manuscript

This article can be cited before page numbers have been issued, to do this please use: C. Pettinari and L. PANDOLFO, *CrystEngComm*, 2017, DOI: 10.1039/C7CE00009J.



This is an Accepted Manuscript, which has been through the Royal Society of Chemistry peer review process and has been accepted for publication.

Accepted Manuscripts are published online shortly after acceptance, before technical editing, formatting and proof reading. Using this free service, authors can make their results available to the community, in citable form, before we publish the edited article. We will replace this Accepted Manuscript with the edited and formatted Advance Article as soon as it is available.

You can find more information about Accepted Manuscripts in the [author guidelines](#).

Please note that technical editing may introduce minor changes to the text and/or graphics, which may alter content. The journal's standard [Terms & Conditions](#) and the ethical guidelines, outlined in our [author and reviewer resource centre](#), still apply. In no event shall the Royal Society of Chemistry be held responsible for any errors or omissions in this Accepted Manuscript or any consequences arising from the use of any information it contains.

# Trinuclear copper(II) pyrazolate compounds: a long story made of serendipitous discoveries and rational design.

Luciano Pandolfo\*<sup>a</sup> and Claudio Pettinari\*<sup>b</sup>

<sup>a</sup> Dipartimento di Scienze Chimiche, Università di Padova, Via Marzolo, 1, I-35131 Padova, Italy.

<sup>b</sup> Scuola di Farmacia, Università di Camerino, Via S. Agostino, 1, I-62032 Camerino (MC), Italy.

## Abstract

In the past decade, a great effort was put into the development of synthetic strategies to produce trinuclear triangular Cu<sup>II</sup> (TTC) arrays, possibly synthetic analogues for the trinuclear site in ascorbate oxidase and blue oxidase. A large number of scientific contributions have been dedicated to the synthesis and spectroscopic characterization of TTC. In contrast, only a small number of studies deal with their possible applications. As a consequence, systematic studies describing their reactivity are very rare and the few existing models are hardly able to explain how structural and molecular parameters influence the reactivity and their possible uses and application. This contribution reports a summary of all experimental results related to Cu<sub>3</sub>(μ<sub>3</sub>-OH)(μ-pz)<sub>3</sub> core (pz = unsubstituted pyrazolate). We describe here all species distinguishing them in neutral, cationic and anionic, their main structural features, the synthetic procedures employed for their production, their reactivity toward nucleophiles and strong acids and, finally, their possible and perspective applications.

## Introduction

Polynuclear copper(II) assemblies continue to attract researcher's attention, mainly due to their possible catalytic activity,<sup>1-10</sup> magnetic properties<sup>11-20</sup> and to the fact that they are present in some naturally occurring metalloproteins, as laccase and ascorbate oxidase, which are able to catalyze the oxidation of specific substrates as polyphenols and aromatic amines in living organisms through the four-electron reduction of atmospheric dioxygen to water.<sup>21-28</sup> Thus, the study of polynuclear copper(II) complexes continues to attract relevant interest and, in this context, the obtaining and characterization of trinuclear triangular Cu<sup>II</sup> arrays have been, and continue to be, the subjects of a huge number of studies. Particularly, numerous trinuclear triangular copper complexes possessing the Cu<sub>3</sub>(μ<sub>3</sub>-OH) core have been reported and structurally characterized. In detail, the CCDC data base returns more than 600 entries where the Cu<sub>3</sub>(μ<sub>3</sub>-OH) core (Chart 1a) is present. In 175 of them any copper ion is further connected by a couple of X donor atoms (X = O or N) belonging to three ditopic ligands (Chart 1b)<sup>29</sup> which often are azolates (129 entries). In most cases bridging ditopic ligands are pyrazolates (87 entries), 76 of which unsubstituted, while in 42 cases tri- or tetra-azolates are involved. Here we will review the most relevant structural features of compounds characterized by the trinuclear assemblies

$\text{Cu}_3(\mu_3\text{-OH})(\mu\text{-pz})_3$  (pz = pyrazolate) (TTC)<sup>5</sup> where copper(II) ions are connected, besides the capping  $\mu_3$ -hydroxido group, by three unsubstituted pyrazolates (Chart 1c). View Article Online  
DOI: 10.1039/C7CE00009J

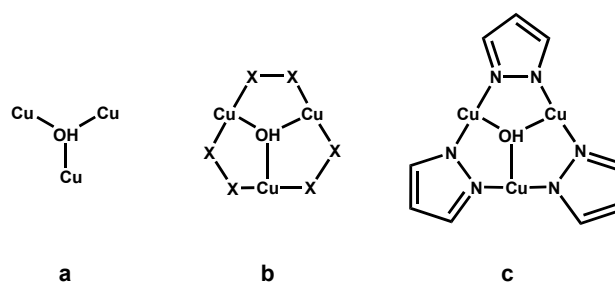


**Chart 1**

First of all, it is to note that, despite the structure shown in Chart 1c seems to have a threefold axis passing through O and perpendicular to the plane defined by the three Cu ions, this feature is actually present only in two compounds, catena-(( $\mu_6$ -benzene-1,3,5-tricarboxylato)-( $\mu_3$ -hydroxido)-( $\mu_3$ -oxido)-hexakis( $\mu$ -pyrazolato)-hexa-copper(II)),<sup>30</sup> **1**,<sup>55</sup> and ( $\mu_3$ -hydroxido)-tris( $\mu$ -pyrazolato-N,N')-tris(1H-pyrazole-N<sup>2</sup>)-tri-copper(II)( $\mu_3$ -oxido)-tris( $\mu$ -pyrazolato-N,N')-tris(1H-pyrazole-N<sup>2</sup>)-tri-copper(II) tris(trifluoromethanesulfonate), **2**.<sup>31</sup> In both compounds a  $\text{Cu}_3(\mu_3\text{-O})(\mu\text{-pz})_3$  moiety is faced to a TTC fragment, (Figure 1) and the threefold axis overlaps the segment joining the oxygen atoms.

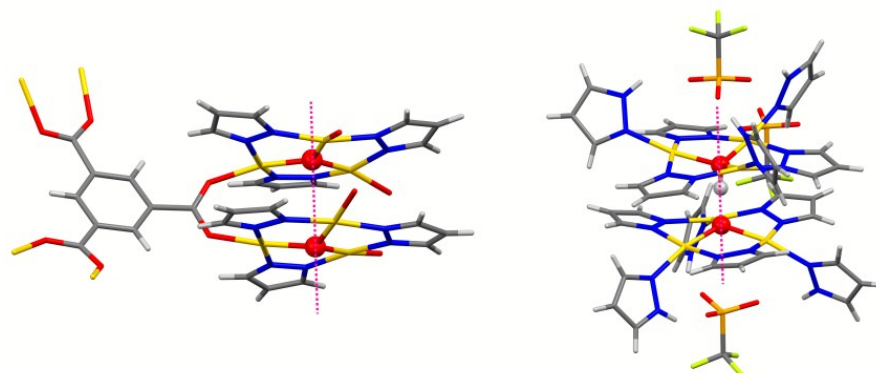


**Figure 1** – Structures of **1** (left) and **2** (right) with the three-fold axes shown as magenta dotted lines.

Anyhow, in all TTC derivatives the oxygen is placed out of the plane determined by the three Cu ions of about 0.2-0.6 Å while, in the  $[\text{Cu}_3(\mu_3\text{-O})]$  moieties the oxygen lies in that plane, as found in all compounds containing this specific fragment, as bis(triphenylphosphine)iminium bis( $\mu_3$ -oxido)-tris( $\mu$ -3,5-diphenylpyrazolato)-hexakis( $\mu$ -pyrazolato)-hexa-copper(II), **3**,<sup>32</sup> tetra-*n*-butylammonium ( $\mu_3$ -oxido)-tris( $\mu$ -pyrazolato-N,N')-(benzoato-O)-tri-copper(II), **4**,<sup>33</sup> and catena-(( $\mu_3$ -oxido)-( $\mu_3$ -pyridine-3,4-dicarboxylato)-tris( $\mu$ -pyrazolato)-diaqua-methanol-tri-copper(II) unknown solvate), **5**.<sup>34</sup> In compound **2** the  $\mu_3\text{-OH}$  group is involved into a strong H-bond with  $\mu_3\text{-O}$  belonging to the second trinuclear moiety (see Figure 1), and this makes  $\mu_3\text{-O}$  enough similar to a  $\mu_3$ -hydroxido moiety, reflecting into the position of oxygen which results placed out of the  $\text{Cu}_3$  plane of about 0.43 Å.

The other relevant geometrical features pertaining to all the structurally characterized TTC moieties are quite normal. Excluding compounds **1** and **2**, in all species copper ions form isosceles or scalene triangles and non-bonding Cu...Cu distances fall between 3.08 and 3.46 Å. Analogously, Cu-O and Cu-N bond distances are included between 1.88-2.08 and 1.86-2.03 Å, respectively.

The TTC fragments are doubly positively charged and this charge can be differently balanced, as schematized in Chart 2 where X indicates a monoanionic species, yielding anionic, neutral or cationic derivatives. Moreover, in few cases, di- or trianionic species are instead present and in almost all the cases copper ions coordinate also neutral molecules as Hpz, water or other solvents or mono or polytopic ligands as pyridine or bipyridine, which are not evidenced in the structures sketched in Chart 2.

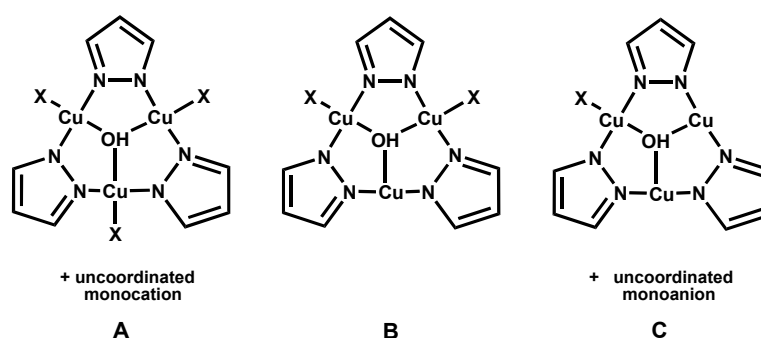


Chart 2

### Ionic species

Considering only ionic species, the CCDC database reports 10 type A and 12 type C compounds. In the case of type A derivatives, the uncoordinated monocation is tetra-*n*-butylammonium (compounds **6-7**,<sup>34</sup> **8-9**,<sup>35</sup> **10**<sup>36</sup> and **11**<sup>37</sup>), triethylammonium (compound **12**<sup>38</sup>), or (triphenylphosphino)iminium (compounds **13**<sup>34</sup> and **14-15**<sup>36</sup>), while in the case of type C the uncoordinated monoanion is chloride (compounds **16**<sup>39</sup> and **17**<sup>40</sup>), hydroxide (compounds **18-21**<sup>41</sup> and **22-23**<sup>42</sup>), trifluoromethanesulfonate (compounds **2**,<sup>31</sup> **24**<sup>37</sup> and **25**<sup>43</sup>) and dicyano(nitro)methanide (compound **26**<sup>44</sup>).

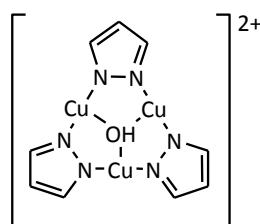
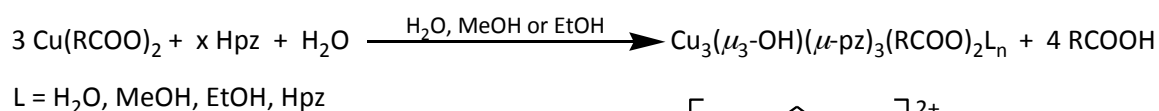
### Neutral species

Type B non-ionic species, where anions are coordinated to copper(II) ions, account for the larger number of compounds containing the TTC fragment, 54 entries. In detail, 18 derivatives bear inorganic anions, actually nitrate (compounds **27**,<sup>31,45</sup> **28**,<sup>31,46</sup> **29**<sup>47</sup> and **30**<sup>48</sup>), chloride (compounds **31-32**,<sup>39</sup> **33**<sup>49</sup> and **34**<sup>50</sup>), bromide, (compound **35**<sup>51</sup>), perchlorate (compounds **36**<sup>31</sup> and **37**<sup>52</sup>), trifluoromethanesulfonate (compounds **38**<sup>31</sup> and **39-41**<sup>43</sup>), sulfate (compound **42**<sup>31</sup>), phosphonate (compound **43**<sup>47</sup>) and sulfate plus nitrate (compound **44**<sup>53</sup>). Organic anions are instead present in 36 cases, actually in derivatives bearing formate (compounds **45-46**<sup>41</sup> and **47**<sup>54</sup>), acetate (compounds **48-49**<sup>42</sup> and **50**<sup>55</sup>), trifluoroacetate (compound **51**<sup>31</sup>), propanoate (compounds **52-53**,<sup>7</sup> **54**<sup>42</sup> and **55**<sup>54</sup>),

butyrate (compound **56**<sup>54</sup>), valerate (compound **57**<sup>56</sup>), hexanoate (compound **58**<sup>56</sup>), heptanoate (compound **59**<sup>56</sup>), acrylate (compounds **60-61**<sup>42</sup> and **62-63**<sup>57</sup>), methacrylate (compound **64**<sup>57</sup>), pivalate (compound **65**<sup>58</sup>), phenylacetate (compound **66**<sup>58</sup>), vinylacetate (compound **67**<sup>58</sup>), phenylpropanoate (compound **68**<sup>58</sup>), cyclohexylcarboxylate (compound **69**<sup>58</sup>), isocyanate (compound **70**<sup>59</sup>), fumarate (compound **71**<sup>60</sup>), 2-methylfumarate (compound **72**<sup>60</sup>), succinate (compounds **73-75**<sup>61</sup>), 2-hydroxynaphthalene-1,4-dicarboxylate (compound **76**<sup>62</sup>), biphenyl-4,4'-dicarboxylate (compound **77**<sup>62</sup>), 3-pyridine-3,4-dicarboxylate (compound **78**<sup>62</sup>), and benzene-1,3,5-tricarboxylate (compound **1**<sup>30</sup>). Moreover, in compound **79**<sup>63</sup> two TTC moieties, which are faced each other and connected through three 3,5-diphenylpyrazolates, encapsulate a fluoride anion.

## Synthetic procedures

The syntheses of compounds containing the TTC fragment has been generally performed by reacting copper(II) salts with Hpz and water, which need to be deprotonated to give pz<sup>-</sup> and OH<sup>-</sup> anions, respectively. In some cases the deprotonation was achieved by adding an exogenous base as NaOH,<sup>34,36,37,43,45,48,52,53</sup> Bu<sub>4</sub>NOH,<sup>35</sup> or Et<sub>3</sub>N.<sup>38,47</sup> When copper salts of weak acids are employed (mono, di or tricarboxylates) the presence of the exogenous base is not needed, since the basicity of carboxylates appears to be adequate to shift the deprotonation equilibria of Hpz and water toward the formation of pz<sup>-</sup> and OH<sup>-</sup> in an amount sufficient to produce the self-assembly of the TTC fragment,<sup>7,9,30,40,54,55,57,58,60-62</sup> according to the reaction depicted in Scheme 1 for a generic monocarboxylate. In few cases the TTC assembly was instead obtained through the aerobic oxidation of copper(I) derivatives, in detail the cyclic trinuclear Cu<sub>3</sub>(μ-pz)<sub>3</sub> species, the mononuclear Cu<sup>I</sup>(Hpz)<sub>2</sub>(NO<sub>3</sub>) and the dinuclear [Cu<sup>I</sup>(Hpz)<sub>2</sub>(Cl)]<sub>2</sub> complexes, yielding the TTC containing compounds **33**,<sup>49</sup> **28**<sup>46</sup> and **34**,<sup>50</sup> respectively.



Scheme 1

## Structural description

### Ionic compounds

The structures of ionic compounds all consist of discrete ionic couples. In the cases of type A derivatives (Chart 2) cations often interact with the anionic TTC fragments through more or less strong non-covalent interactions, as shown in Figure 2, where are reported the structures of compounds **7**<sup>34</sup> (left)

and **12**<sup>38</sup>. In **7** N-H<sub>ammonium</sub>...Cl, N-H<sub>pyrazole</sub>...Cl and O-H...Cl H-bonds generate a 1D supramolecular network, while in **12** two quite strong N-H...O H-bonds connect two ammonium cations to a hexanuclear motif obtained through two, symmetry equivalent, monatomic O acetate bridges.

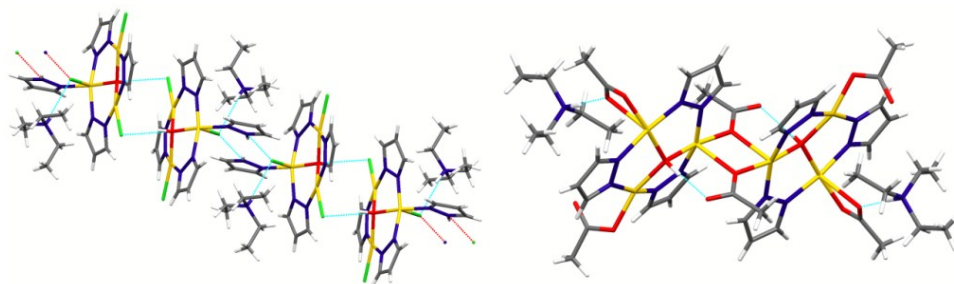


**Figure 2** – Structures of **7** (left) and **12** (right), where crystallization benzene molecules have been removed for clarity.<sup>555</sup>

Similar supramolecular interactions are present also in type C compounds (Chart 2). As an example, in Figure 3 compound **16**<sup>39</sup> is shown, where Cl<sup>-</sup> ions interact with N-H<sub>pyrazole</sub> fragments belonging to a hexanuclear system generated, analogously to **12**, by two, symmetry equivalent, monatomic O acetate bridges connecting two TTC units. Incidentally, also in this case two quite strong, O-H...O bonds likely reinforce the hexanuclear assembly.

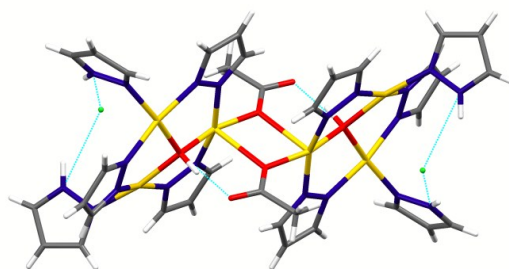


**Figure 3** – Molecular structure of **16**. Crystallization water molecules have been removed for clarity.

A series of H-bonds involving  $\mu_3$ -OH, coordinated and crystallization water, coordinated chloride ions and ionic dicyano(nitro)methanide, generating an extended 2D supramolecular network (Figure 4), constitutes a relevant issue also in the case of the ionic TTC compound **26**.<sup>44</sup>

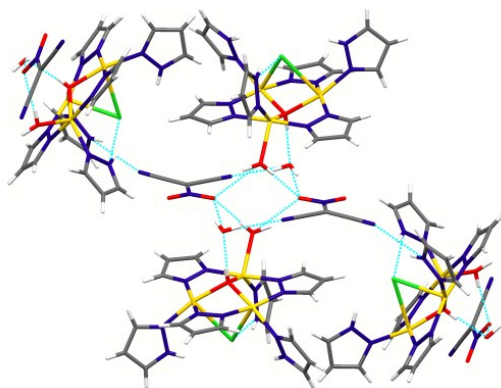


**Figure 4** – H-bonds connecting four trinuclear cationic moieties in **26**.

## Non-ionic compounds

### Inorganic counterions

In non-ionic TTC species (type B compounds, Chart 2), sometimes we found coordinated inorganic ions that may behave as mono or polytopic ligands generating isolated trinuclear species, hexanuclear assemblies or Coordination Polymers (CPs) where the TTC moiety acts as a Secondary Building Unit (SBU).<sup>64</sup> Interestingly, the inorganic anion seems to be scarcely relevant in the determination of the kind of assembly, as witnessed, for example, by the obtaining of four distinct compounds (**29**,<sup>47</sup> **27**,<sup>31,45</sup> **30**<sup>48</sup> and **28**<sup>31,46</sup>) (see Figure 5), all based on the same  $\text{Cu}_3(\mu_3\text{-OH})(\mu\text{-pz})_3(\text{NO}_3)_2$  core and differing for the kind and number of ancillary ligands coordinated to Cu ions.

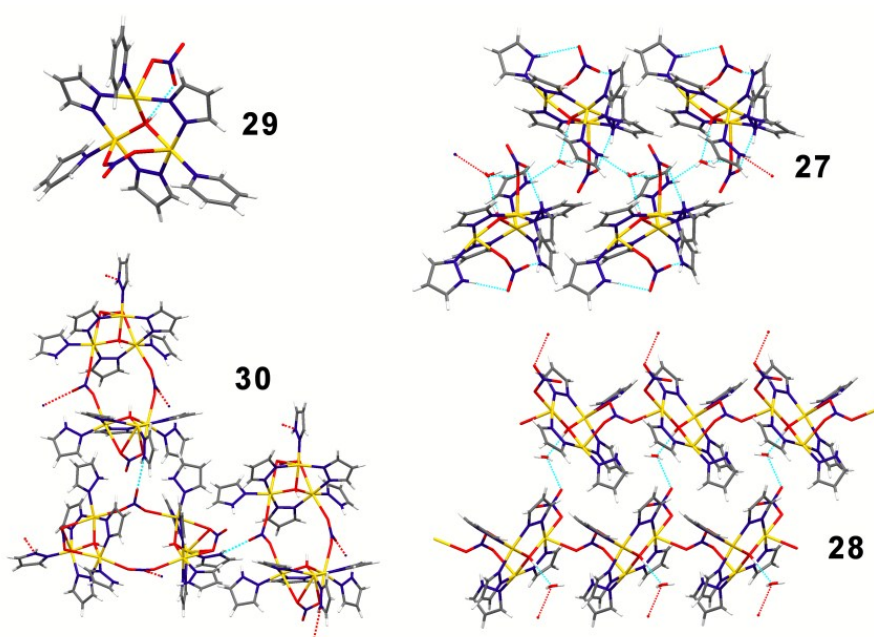


**Figure 5** – Different assemblies of the  $\text{Cu}_3(\mu_3\text{-OH})(\mu\text{-pz})_3(\text{NO}_3)_2$  core.

In compound **29** the presence of three coordinated bulky pyridine molecules probably does not allow the supramolecular assembly of two or more TTC units, and a similar behavior is also present in the case of compound **27** where four coordinated pyrazole molecules likely hamper the direct supramolecular assembly of the TTC moieties. On the other hand, in this case, the presence of a relevant number of  $\text{N-H}_{\text{pyrazole}}$ ,  $\mu_3\text{-OH}$  and crystallization water molecules generates, through quite strong H-bonds, a *zig-zag* 1D supramolecular tape. When only three pyrazole molecules are coordinated to Cu ions of the  $\text{Cu}_3(\mu_3\text{-OH})(\mu\text{-pz})_3(\text{NO}_3)_2$  system (compound **30**), symmetry equivalent  $\text{NO}_3^-$  ions act as ditopic ligands generating hexanuclear assemblies, which are further connected each other through H-bonds, forming a 2D supramolecular network. Finally, since in compound **28** each TTC unit bears only two coordinated pyrazole molecules, possibly there is room enough to permit, through

$\text{NO}_3^-$  bridges joining the TTC SBUs, the formation of 1D CPs which are further connected through H-bonds involving also crystallization water molecules and generate a 2D supramolecular network. Other interesting examples of neutral TTC species containing coordinated inorganic anions have been reported. As an example, while in the trifluoromethanesulfonate TTC derivative **38**<sup>31</sup> only inter- and intra-molecular H-bonds involving crystallization water molecules are present, leading to the supramolecular hexanuclear cluster shown in Figure 6, a hexanuclear species having a structure very similar to that of compound **30** is formed in the perchlorate derivative **37** (Figure 7), where  $\text{H}\cdots\text{O}_{\text{perchlorate}}$  and  $\text{O}-\text{H}\cdots\text{O}_{\text{perchlorate}}$  H-bonds likely reinforce the hexanuclear assembly.<sup>31</sup>

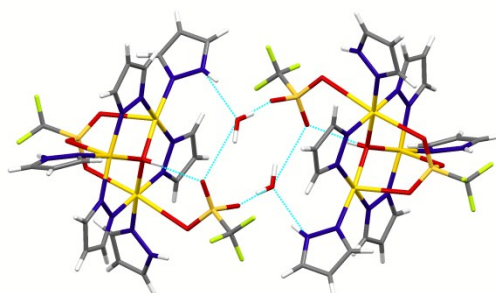


**Figure 6** – Hexanuclear supramolecular assembly of **38** obtained through H-bonds.

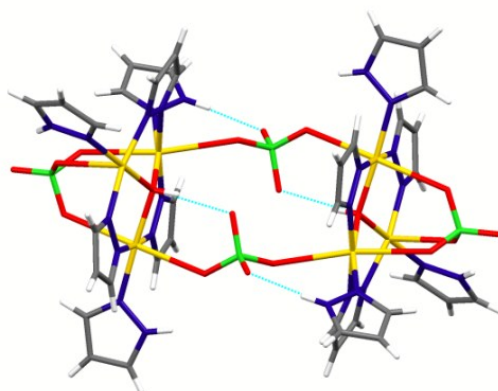


**Figure 7** – The hexanuclear cluster of **37**.

A 1D CP is instead formed in the case of compound **42**, where the sulfate dianion bridges two trinuclear units, as shown in Figure 8. In this case the H-bonds likely participate to the stabilization of the polymeric assembly.<sup>31</sup>

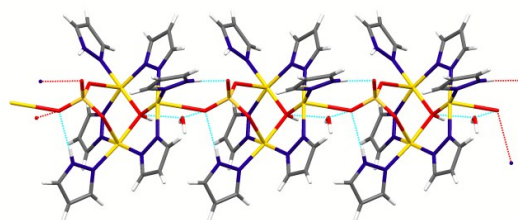


**Figure 8** – The 1D CP in the crystal structure of **42**.



An intriguing assembly is present in compound **44**, where two different anions are present, namely nitrate and sulfate.<sup>53</sup> The ditopic behavior of  $\text{NO}_3^-$  coupled to the hexatopic one of  $\text{SO}_4^{2-}$  generates the peculiar 1D CP shown in Figure 9.

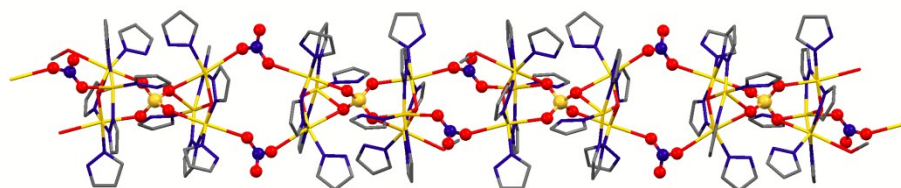


**Figure 9** – The 1D CP of **44** generated through the alternating bridging of sulfate and nitrate ions (ball-and-stick representation). H atoms, crystallization MeCN and water molecules have been removed for clarity.

The ditopic behavior of bromide ions coordinated to the TTC clusters of compound **35** generates 8-membered and 20-membered metallacycles which self-assemble forming a 2D CP<sup>51</sup> which is partly shown in Figure 10.

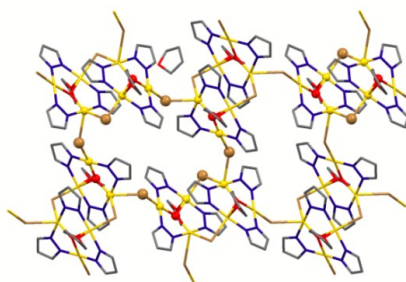


**Figure 10** – The 2D CP of **35** generated by cumulated 8- and 20-membered metallacycles (two of them are evidenced by ball-and-stick representation). H atoms and crystallization THF molecules have been removed for clarity.

### Organic counterions

When the anions balancing the double positive charge of the TTC core are coordinated carboxylates particularly relevant features, due to carboxylate polytopic behavior, are often present. Actually, coordinated monocarboxylates reported in Table 1 generate hexa- or dodecanuclear assemblies or 1- or 2D CPs.

Table 1 – Polytopic monocarboxylates generating hexa- or dodecanuclear assemblies or 1- or 2D CPs in

CrystEngComm Online  
DOI: 10.1039/C7CE00009J

TTC compounds.

Anion <sup>(a)</sup>	TTC, assembly	Ref.	Anion	TTC, assembly	Ref.
formate	<b>47</b> , 1D CP	54	methacrylate	<b>64</b> , 1D CP	57
acetate	<b>50</b> , 2D CP	55	phenylacetate	<b>66</b> , 1D CP	58
propanoate	<b>55</b> , 1D CP	54	vinylacetate	<b>67</b> , 1D CP	58
butyrate	<b>56</b> , hexa	54	phenylpropanoate	<b>68</b> , dodeca	58
acrylate	<b>62</b> , hexa, <b>63</b> , 1D CP	57	cyclohexylcarboxylate	<b>69</b> , 1D CP	58

<sup>(a)</sup> In some cases (valerate, 2-methylbutyrate, hexanoate and heptanoate derivatives) the presence of the trinuclear triangular structure was inferred from other physico-chemical determinations and the possible further assembly was not defined.<sup>9</sup>

More specifically, in compound **50**<sup>55</sup> two acetate ions displaying a ditopic and a tritopic behavior act, respectively, as bridges connecting three trinuclear units, thus generating cumulated 28-membered metallacycles which, as a sort of Tertiary Building Units, are the bricks of waved 2D sheets (Figure 11).

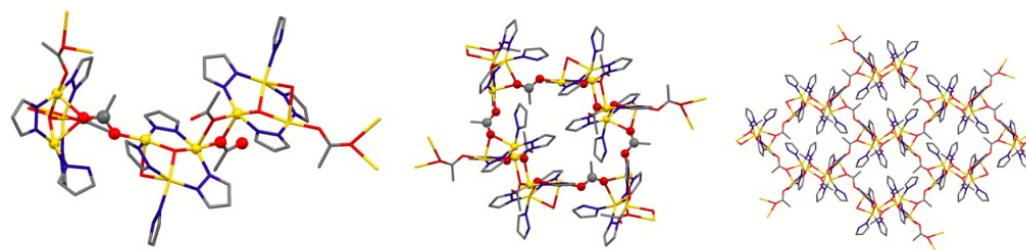


**Figure 11** – Left: self-assembly of three trinuclear units of compound **50**. Center: one of the 28-membered metallacycles obtained through acetates connections. Right: four cumulated metallacycles define part of a waved 2D CP. H atoms have been removed for clarity.

Even though the obtaining of the trinuclear triangular assembly is a common feature in the reaction of copper(II) carboxylates ( $\text{Cu}(\text{RCOO})_2$ ) with Hpz and water in protic media (provided that  $\text{RCOO}^-$  is a base strong enough to efficiently deprotonate water and Hpz), it is quite difficult to forecast the possible assemblies of these hydroxidoclusters, that seem to depend not only from the structure and steric hindrance of R, but also from the syntheses conditions, as reaction ratios, solvent or temperature. As an example, by reacting at rt copper propanoate (in EtOH) and copper acrylate (in MeOH) with Hpz and traces of water, TTC derivatives **55**<sup>54</sup> and **63**<sup>57</sup> have been obtained, respectively. The structures of the two asymmetric units are almost superimposable, being the most relevant difference due to the coordination of EtOH in **55** and MeOH in **63** (Figure 12).

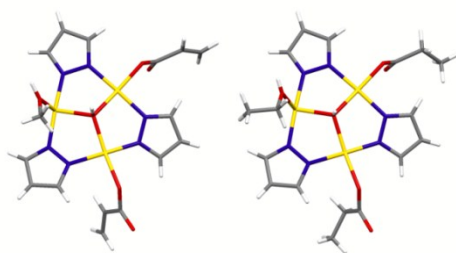


**Figure 12** – Asymmetric units of **63** (left) and **55** (right).

Moreover, in both cases carboxylates behave as ditopic ligands, thus the TTC units are linked through two monatomic and two *syn-syn* bridges, generating 1D CPs whose structures are almost superimposable too (Figure 13).

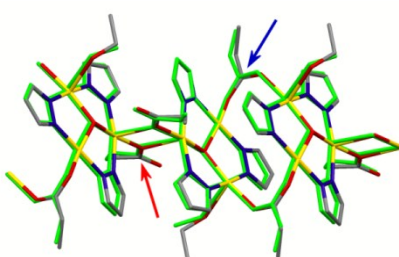


**Figure 13** – The 1D CPs generated by monatomic (red arrow) and *syn-syn* bridges (blue arrow) in **55** (structure shown in green color) and **63**. H atoms have been removed for clarity.

While the above results are reasonably expected, due to the similarity of propanoate and acrylate chains, it is to note that in some cases even small changes in the synthetic procedures may generate large differences in the further assembly of the trinuclear clusters. As an example, even though the synthetic procedures leading to the two acrylate derivatives **63** and **62** (Hpz:copper acrylate = 1.2, solvent MeOH for **63** and Hpz:copper acrylate = 1.35, solvent H<sub>2</sub>O for **62**) are very similar nevertheless, **62** displays relevant differences compared to **63**.<sup>57</sup> Beside water, each trinuclear cluster of **62** coordinates also a molecule of Hpz and one carboxylate ion has a chelating coordination while only the second one acts as a ditopic ligand (monatomic bridging), thus generating the hexanuclear assembly shown in Figure 14. Incidentally, an analogous hexanuclear island, **56**, was obtained from the reaction of copper butyrate with pyrazole in water, followed by recrystallization in MeOH.<sup>54</sup>

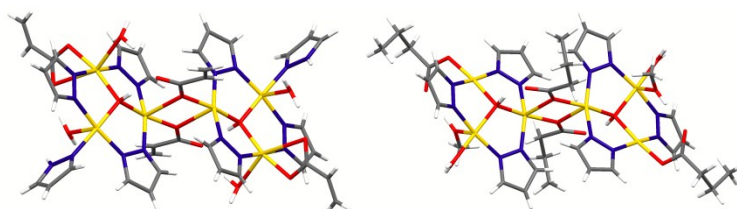


**Figure 14** – The hexanuclear assemblies of **62** (left) and **56** (right).

The influence of, seemingly unimportant, different reaction conditions on the assembly of the TTC fragment is further put in evidence by the synthesis of the propanoate based TTC derivatives **53** and **52**<sup>7</sup> (Figure 15).

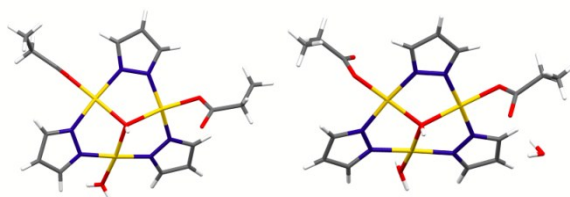


**Figure 15** – Molecular structures of **53** (left) and **52** (right).

These compounds differ only for a crystallization water molecule, which is present only in **52**. They were obtained by reacting copper propanoate in water and, contrarily to compound **55** that was synthesized in EtOH,<sup>54</sup> they do not assemble to form CPs, due to the monotopic coordination of propanoate ions. Interestingly, the difference in the synthetic procedure leading to **52** and **53** consists only on the final crystallization process, which was carried out in the 18-22 °C range for **53**, while **52** was recrystallized at 10-14 °C. It is suggestive to suppose that a little bit lower crystallization temperature is able “to freeze” a water molecule in the lattice of **52**. Moreover, the presence of a further crystallization water molecule produces large differences in the supramolecular assemblies of **53** and **52**. In **52** strong H-bonds involving coordinated and crystallization water molecules, as well as propanoate oxygens, connect the TTC assemblies generating parallel, almost cylindrical, helixes running alternatively clock- and counterclockwise (Figure 16, left). H-bonds drive the supramolecular assembly also of compound **53**, but in this case two 1D, symmetry related supramolecular networks formed, which are further connected, through other H-bonds, leading to the 1D supramolecular tape shown in Figure 16, right.

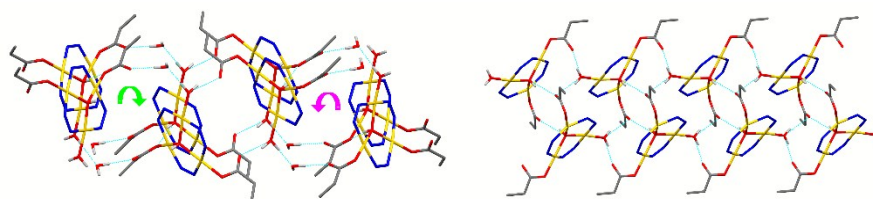
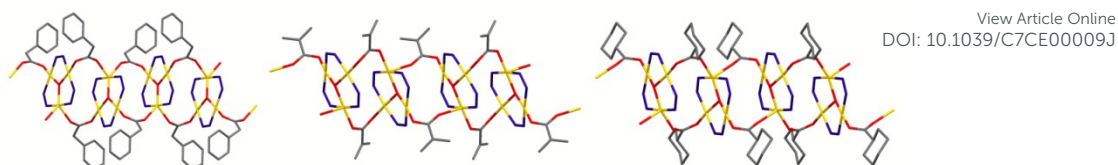


**Figure 16** – Supramolecular assemblies of **52** (left) and **53** (right). Pyrazolate carbon atoms and carbon bonded H atoms have been removed for clarity.

Other peculiar assemblies can be found in TTC derivatives having monocarboxylates as charge balancing ligands. In the methacrylate, cyclohexylcarboxylate and phenylacetate derivatives (compounds **64**,<sup>57</sup> **69**<sup>58</sup> and **66**,<sup>58</sup> respectively) carboxylates double connect two TTC moieties forming 12-membered metallacycles leading to 1D CPs. The differences among these CPS lie in the fact that in **66** both phenylacetates connect the TTC units in a *syn-syn* fashion, while in the other two cases one *syn-syn* and one *syn-anti* connections are present (Figure 17).



View Article Online  
DOI: 10.1039/C7CE00009J

**Figure 17** – 1D CPs assemblies of phenylacetate (**66**) (left), methacrylate (**64**) (center) and cyclohexylcarboxylate (**69**) (right) TTC derivatives. H atoms and pyrazolate carbon atoms have been removed for clarity.

A different kind of 1D CPs has been found in the structure of vinylacetate TTC derivative **67**,<sup>58</sup> where one vinylacetate anion joins two TTC units through a monatomic bridge, while the other one displays a *syn-syn* plus monatomic tritopic behavior, as shown in Figure 18.

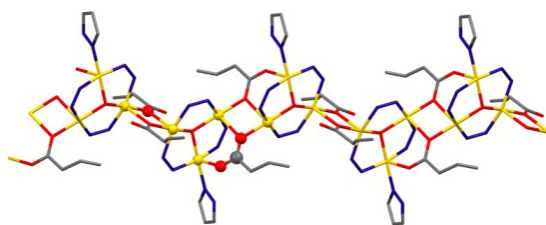


**Figure 18** – The 1D CPs assembly in the vinylacetate based TTC **67**. Monatomic and *syn-syn* plus monatomic coordination are evidenced through ball-and-stick representation. H atoms and pyrazolate carbon atoms have been removed for clarity.

Interestingly, the coordination modes found in the vinylacetate TTC **67** are present also in the case of phenylpropanoate TTC derivative **68**,<sup>58</sup> but in this case only four trinuclear units are connected through two monatomic and two *syn-syn* plus monatomic bridges, yielding a dodecanuclear assembly which is capped by two coordinated water molecules (Figure 19).

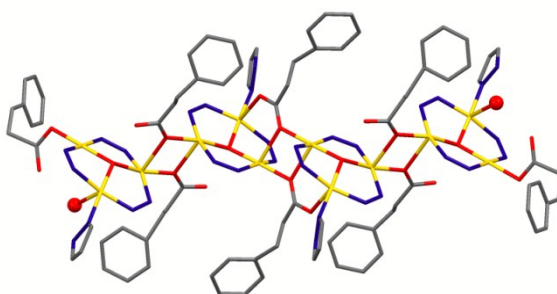


**Figure 19** – The dodecanuclear assembly present in the phenylpropanoate TTC derivative **68**. Capping water molecules (see text) are evidenced by ball-and-stick representation. H atoms and pyrazolate carbon atoms have been removed for clarity.

As above evidenced most of the monocarboxylates lead to the formation of 1D or 2D CPs having the TTC moiety as SBU, and this feature is, *a fortiori*, found when di- or tricarboxylates are employed, as summarized in Table 2.

Table 2 – Di- and tricarboxylates generating 2- or 3D CPs.

Anion	TTC, assembly	Ref.
fumarate	<b>71</b> , 2D CP	60
2-methylfumarate	<b>72</b> , 2D CP	60
succinate	<b>73, 74, 75</b> , 3D CPs	61
2-hydroxynaphthalene-1,4-dicarboxylate	<b>76</b> , 3D CP	62
biphenyl-4,4'-dicarboxylate	<b>77</b> , 3D CP	62
3-pyridine-3,4-dicarboxylate	<b>78</b> , 3D CP	62
benzene-1,3,5-tricarboxylate	<b>1</b> , 3D CP	30

In detail, the hydrothermal reaction of copper fumarate or 2-methylfumarate with pyrazole yielded the isomorphous derivatives  $\text{Cu}_3(\mu_3\text{-OH})(\mu\text{-pz})_3(\text{fumarate})(\text{Hpz})$ , **71**, and  $\text{Cu}_3(\mu_3\text{-OH})(\mu\text{-pz})_3(\text{methylfumarate})(\text{Hpz})$ , **72**.<sup>60</sup> In Figure 20 is reported the molecular structure of **71** and the 2D CP obtained through the fumarate connections. The isomorphous derivative **72** displays almost the same geometrical parameters.

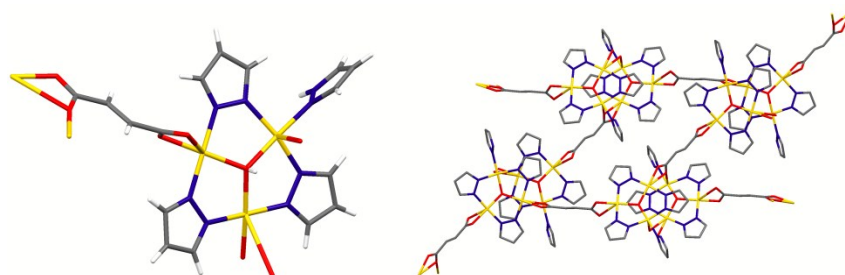
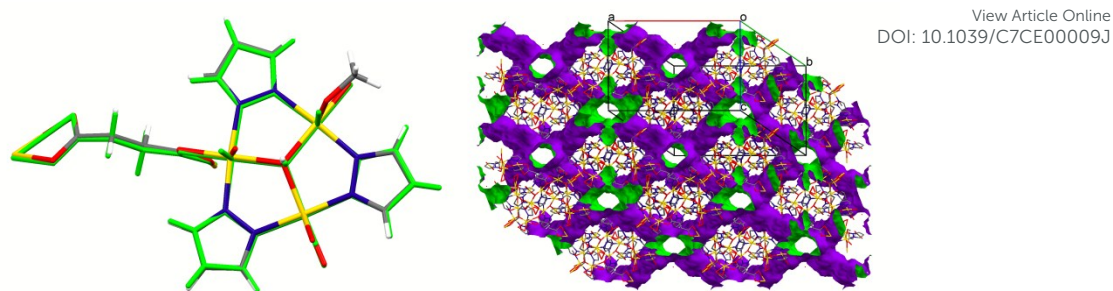


**Figure 20** – The molecular structure of the fumarate TTC **71** (left) and the 2D CP obtained through the polytopic coordination of fumarate ions (right). H atoms have been removed for clarity.

When the “flexible” succinate was employed instead of a “rigid” carboxylate as fumarate or 2-methylfumarate three different CPs, **73**, **74** and **75** were isolated.<sup>61</sup> Compound **74**,  $[\text{Cu}_3(\mu_3\text{-OH})(\mu\text{-pz})_3(\text{succinate})(\text{H}_2\text{O})_{2.5}] \cdot x\text{H}_2\text{O} \cdot y\text{MeOH}$ , was obtained from a solvothermal reaction of sodium succinate, Hpz and copper sulfate in MeOH/H<sub>2</sub>O and a distinct, serendipitous, reaction yielded compound **73**,  $[\text{Cu}_3(\mu_3\text{-OH})(\mu\text{-pz})_3(\text{succinate})(\text{H}_2\text{O})(\text{MeOH})] \cdot \text{H}_2\text{O}$ . Compounds **74** and **73** crystallize in the same space group with almost identical cell parameters. In Figure 21 (left) is evident that the two structures are almost exactly superimposable. In both cases succinate ions bridge the trinuclear fragments in a quite complex way, generating 3D porous CPs (about 20% solvent accessible void space). In Figure 21 (right) is shown the crystal lattice of **73**, evidencing the porosity of this compound.



View Article Online  
DOI: 10.1039/C7CE00009J

**Figure 21** – On the left the superimposed structures of **74** (green color) and **73**. On the right, crystal lattice of **73** showing the porosity of this compound. Inside and outside pore walls are displayed in green and violet colors, respectively. Crystallization water and MeOH molecules have been omitted for clarity.

When compounds **74** or **73** were dried under vacuum at rt, not only crystallization, but also coordinated water and MeOH were easily removed, yielding the TTC derivative  $[\text{Cu}_3(\mu_3\text{-OH})(\mu\text{-pz})_3(\text{Succinate})]$ , **75**, that was also obtained through a hydrothermal reaction of copper succinate with Hpz.<sup>61</sup> The structure of **75**, displayed in Figure 22 (left), evidences some similarity with those of **74** and **73**, but also some differences, mainly in the orientation of the succinate carbons chain, that very likely is responsible of (or *vice-versa* is due to) the different assembly of the TTC units. Carboxylate moieties of each succinate display different (*syn-syn* and *syn-anti*) bridging modes, generating distinct 12-membered metallacycles that are connected through the  $\text{C}_2$  succinate chains, yielding a non-porous 3D CP.

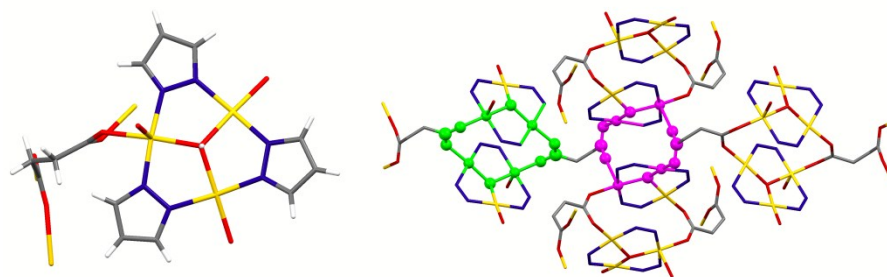


**Figure 22** – Molecular structure of **75** (left). On the right the succinate chain joins two different 12-membered metallacycles formed through *syn-syn* (green) and *syn-anti* (magenta) COO bridging connections, generating a 3D CP. H atoms and pyrazolate carbon atoms are omitted for clarity.

Other dicarboxylates were employed in the synthesis of TTC derivatives, 2-hydroxynaphthalene-1,4-bicarboxylate, biphenyl-4,4'-bicarboxylate and 3-pyridine-3,4-bicarboxylate, which yielded the 2D CP **76** and two 3D CPs (**78** and **77**), respectively,<sup>62</sup> whose structures are shown in Figure 23. Each 2D sheet of compound **76** presents evident pores; however, being the parallel sheets arranged offset, no effective porosity is present. On the contrary, compounds **78** and **77** display true, not connected pores or parallel channels accounting for about 22% and 38% solvent accessible void space, respectively.

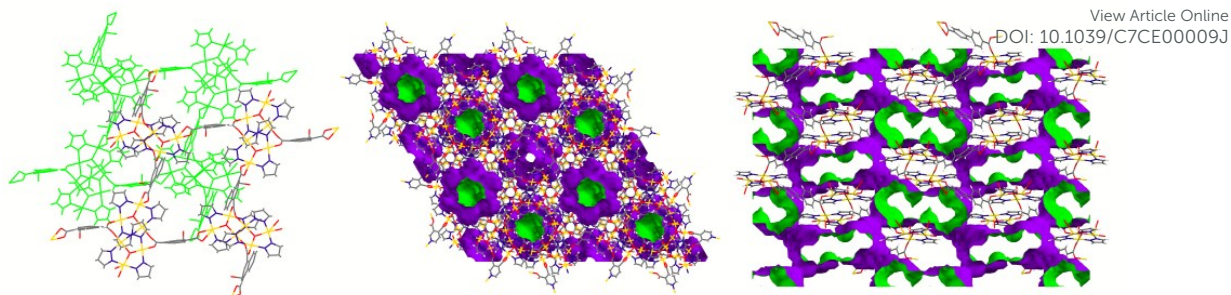


**Figure 23** – The structure of **76** (left), where two staggered 2D CPs are displayed with different colors. In the crystal lattices of **78** (center) and **77** (right) inside and outside pore walls are evidenced with green and violet colors, respectively.

Finally, the solvothermal reaction of copper nitrate, Hpz and benzene-1,3,5-tricarboxylic acid yielded the already shortly discussed derivative **1**<sup>30</sup> where each tricarboxylate connects three hexanuclear units (Figure 24), resulting in an interpenetrated 3D CP.

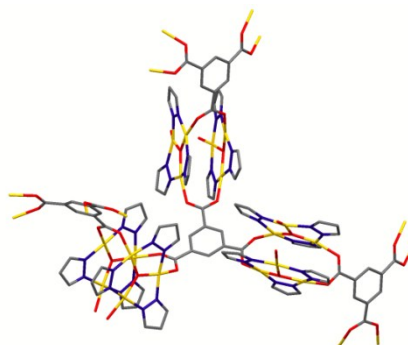


**Figure 24** – The structure of **1** evidencing how benzene-1,3,5-tricarboxylate bridges three couples of trinuclear units. H atoms have been removed for clarity.

## Reactivity

### Reactions with strong acids

From all literature data it appears evident that even though different synthetic procedures are employed (for example, the solvothermal or ambient reaction conditions, the presence of exogenous bases or the use of copper carboxylates) the TTC derivatives self-assemble quite easily, possibly suggesting a good stability of the TTC metallacycle. This assumption is reinforced by the results of the reaction of the acetate based TTC derivative **50**<sup>55</sup> with some strong acids. Actually, by reacting **50** with a water solution of HCl,<sup>39</sup> besides the mononuclear species  $\text{Cu}(\text{Cl})_2(\text{HPz})_4$ , resulting from a partial decomposition, two hexanuclear derivatives also formed, the already mentioned compound **16** (see Figure 3) and compound **32**, where one or two acetates of **50** are replaced by chloride anion(s), respectively. In compound **32** H-bonds connect the hexanuclear island forming a 2D supramolecular network, partly shown in Figure 25.



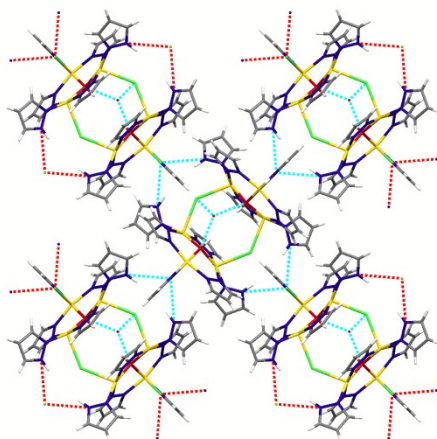


**Figure 25** – The H-bonds driven 2D supramolecular assembly present in **32**.

From the reaction of **50** with HCl also a heptanuclear derivative, **31**, formed,<sup>39</sup> where two  $\text{Cu}_3(\mu_3\text{-OH})(\mu\text{-pz})_3(\text{Cl})_2(\text{Hpz})_2(\text{H}_2\text{O})$  moieties are weakly bridged through the mononuclear  $\text{Cu}(\text{Cl})_2(\text{Hpz})_2$  fragment (see Figure 26, left). This weak interaction, associated to the ditopic behavior of one chloride ion coordinated to the TTC moiety and to H-bonds involving Cl and  $\mu_3\text{-OH}$  fragments, generates 2D supramolecular assemblies where pores are present. Moreover, these parallel sheets exactly match, forming small, star-shaped, channels accounting for about 8% solvent accessible void space (Figure 26, right).

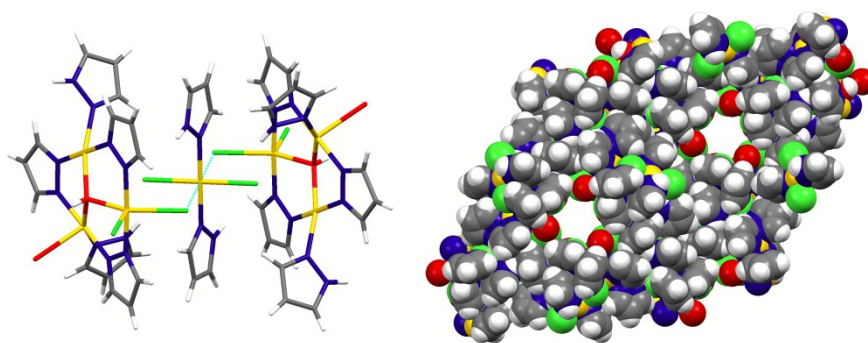


**Figure 26** – The heptanuclear structure of **31** (left). Weak  $\text{Cu}\cdots\text{Cl}$  interactions are represented by cyan dotted lines. On the right: space-fill view down the crystallographic  $c$  axis of the crystal lattice of **31** evidencing star-shaped channels.

Compound **50** was reacted with other strong acids with similar results.<sup>31</sup> In all cases a partial decomposition of the trinuclear unit, leading to the formation of mononuclear pyrazole derivatives, was observed. However, also TTC derivatives formed. In detail, the reaction with  $\text{H}_2\text{SO}_4$  yielded the 1D CP **42**, whose structure has been shown in Figure 8, while the reaction with  $\text{HClO}_4$  generated the hexanuclear islands **37** reported in Figure 7. The reaction of **50** with  $\text{HNO}_3$  yielded two derivatives,<sup>31</sup> the TTC species **27** and the 1D CP **28** reported in Figure 5, which were previously synthesized through

completely different procedures.<sup>45,46</sup> Moreover, from the reaction of **50** with  $\text{CF}_3\text{COOH}$ <sup>31</sup> the TTC derivative **51** was obtained (see Figure 27), while the reaction with  $\text{CF}_3\text{SO}_3\text{H}$  generated two different compounds, the hexanuclear species **2**, whose structure is shown in Figure 1 and the TTC species **38**<sup>31</sup> reported in Figure 6.

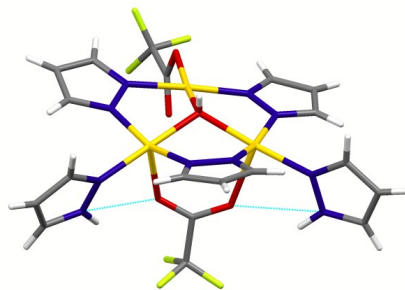


**Figure 27** – Molecular structure of **51**.

Finally, from the reaction of copper chloroacetate with Hpz, the dichloride hexanuclear cluster **17** formed,<sup>40</sup> which exhibits a structure almost superimposable to that of the previously discussed compound **16** (Figure 28). As said above, the reaction of copper carboxylates with Hpz results in the spontaneous self-assembly of the TTC fragment, provided that the carboxylate is basic enough to efficiently deprotonate water and Hpz, as evidenced, for example, by the failure to obtain the TTC moiety in the reaction of copper trifluoroacetate ( $\text{pKb}_{\text{CF}_3\text{COO}} = 13.48$ ).<sup>55</sup> In the reaction of copper chloroacetate ( $\text{pKb}_{\text{ClCH}_2\text{COO}} = 11.13$ ) with Hpz<sup>40</sup> it was observed the formation of a mononuclear 1D CP,  $[\text{Cu}(\text{ClCH}_2\text{COO})_2(\text{Hpz})_2]$ , and of a tetranuclear derivative  $[\{\text{Cu}_2(\mu\text{-pz})(\mu\text{-OCH}_2\text{COO})(\text{Hpz})(\text{MeOH})\}_2(\mu\text{-ClCH}_2\text{COO})_2]$ , the latter obtained through an intramolecular dehydrochlorination reaction. The HCl released in this stage evidently attacked a (not isolated) hexanuclear species generating compound **17**, analogously to what happens in the reaction of **50** with HCl, yielding compound **16**.<sup>39</sup> The formation, in this reaction, of both  $[\text{Cu}(\text{ClCH}_2\text{COO})_2(\text{Hpz})_2]$  and **17** evidences that the  $\text{pKb}_{\text{ClCH}_2\text{COO}}$  lies borderline between the values leading to the exclusive formation of mono and trinuclear species.

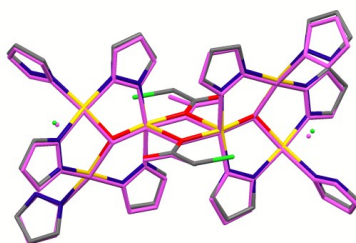


**Figure 28** – The superimposed structures of **16** (evidenced in magenta color) and **17**. H atoms and crystallization water molecules of **16** have been omitted for clarity.

## Reactions with nucleophiles

Besides the reaction with strong acids, the TTC moiety tolerates also nucleophilic attacks and it is possible to treat TTC derivatives with nucleophiles (Nu) obtaining the addition of Nu or the exchange of a pre-existent ligand with Nu. For example, by reacting the trinuclear compound  $[\text{Cu}_3(\mu_3\text{-OH})(\mu\text{-pz})_3(\text{Cl})_2(\text{Hpz})_2]\cdot\text{solv}$  [solv = H<sub>2</sub>O or THF] with pyridine (py), the TTC  $[\text{Cu}_3(\mu_3\text{-OH})(\mu\text{-pz})_3(\text{Cl})(\mu\text{-Cl})(\text{py})_2]\cdot\text{py}$  derivative **34** was easily obtained.<sup>50</sup> The reaction with nucleophiles has been largely exploited by using the ditopic 4,4'-bipyridine (bpy) to connect the TTC moieties with the aim to obtain 1-, 2- or 3D CPs. In one case bpy was employed directly during the synthetic procedure aiming to obtain the TTC moiety. Actually, by reacting  $\text{Cu}(\text{CF}_3\text{SO}_3)_2$  with Hpz, NaOH and py<sup>43</sup> the TTC complex  $[\text{Cu}_3(\mu_3\text{-OH})(\mu\text{-pz})_3(\text{CF}_3\text{SO}_3)(\mu\text{-CF}_3\text{SO}_3)(\text{py})_3]\cdot 0.5\text{H}_2\text{O}$ , **39**, was obtained while, by adding also bpy and tuning the py/bpy ratio, it was possible to isolate the hexanuclear assembly, **40**, the 1D CP **41** and the interpenetrated 3D CP **25** (Figure 29).

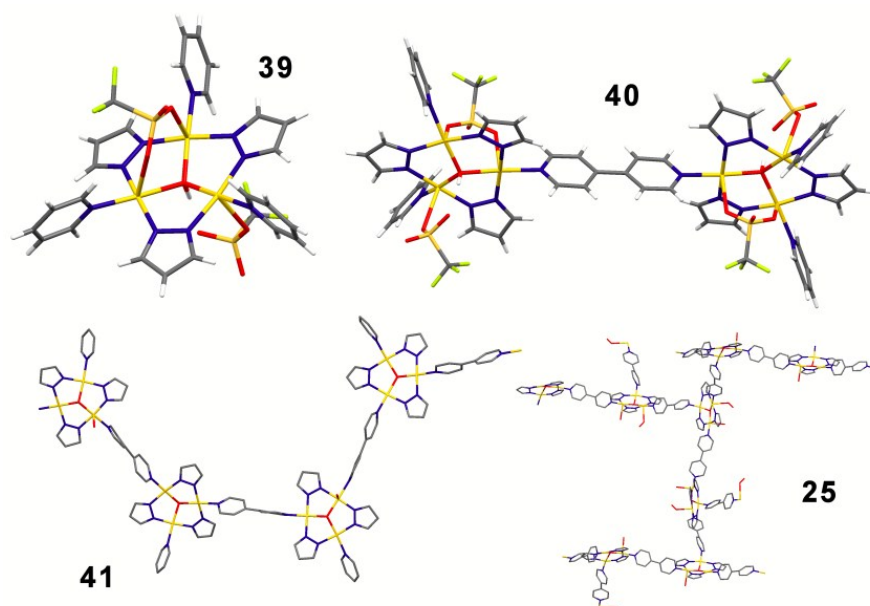


**Figure 29** – The TTC complex **39**, the bpy bridged hexanuclear derivative **40**, part of the 1D CP of **41** and part of the interpenetrated 3D CP of **25**. In compounds **41** and **25** H atoms and  $\text{CF}_3\text{SO}_3$  moieties have been omitted for clarity.

In most cases bpy was instead added to pre-formed trinuclear species. By treating methanol solutions of the formate based TTC **47**<sup>54</sup> with bpy, different compounds were obtained.<sup>41</sup> When the bpy/ $\text{Cu}_3$  ratio was equal to 1, bpy displaced Hpz coordinated to copper in **47** and formed 1D tapes of compound **45** by connecting two 1D CPs (Figure 30). Other weak coordinative interactions among these tapes generate a supramolecular 3D network.

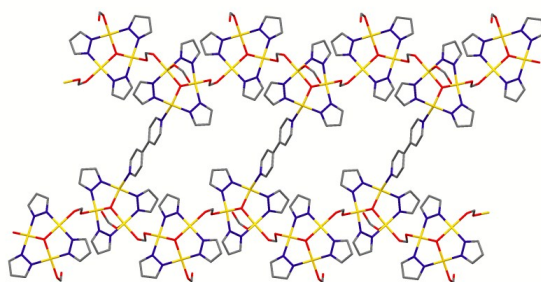


**Figure 30** – 1D tape generated through bpy connections in **45**. Coordinated and crystallization water molecules and H atoms have been removed for clarity.

By using a higher bpy/Cu<sub>3</sub> ratio<sup>41</sup> a formate anion was also displaced from **47** and it was replaced by an uncoordinated hydroxide ion, likely coming from adventitious water, generating the hexanuclear species **18** shown in Figure 31. In compound **18** each TTC unit coordinates three bpy molecules, two of them acting as monotopic ligands, the third one connecting two TTC fragments. A series of strong H-bonds generates a 3D supramolecular network where two different channels are present, one of which partly occupied by further crystallization bpy molecules, accounting for about 23% solvent accessible void space.

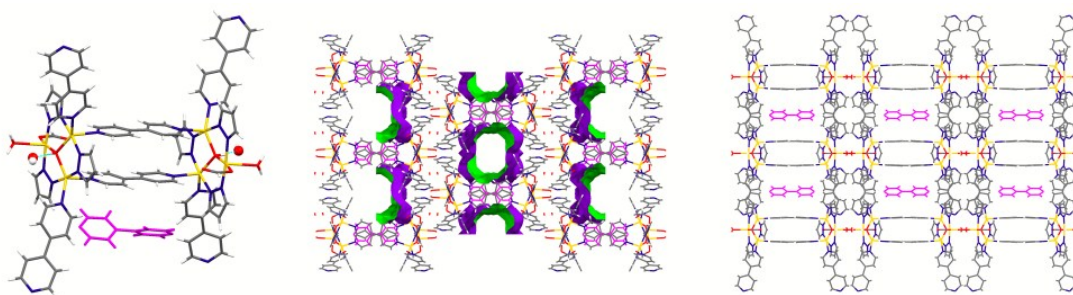
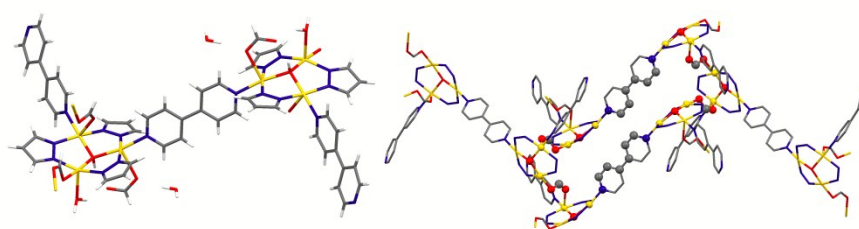


**Figure 31** – On the left the hexanuclear species **18**, where uncoordinated OH anions are evidenced by ball-and-stick representation; view down the *c* (center) and *b* (right) crystallographic axes of the supramolecular 3D network of **18**. Crystallization bpy molecules are evidenced in magenta color, while inside and outside pore surfaces are displayed with green and violet colors, respectively.

Interestingly, crystals of **18** soaked in benzene, toluene or cyclohexane, lost crystallization bpy molecules that were replaced by these solvents, maintaining the original crystalline habit and almost identical cell parameters. On the other hand, if dissolved in MeOH **18** decomposed yielding, besides the trinuclear triangular species **80** where the  $\mu_3$ -OH group is substituted by the  $\mu_3$ -OMe fragment, the above described species **45** and the **46** derivative. The latter consists in two TTC moieties joined through a ditopic bpy (Figure 32, left); moreover each trinuclear fragment coordinates two formate anions, one of which acts as a monatomic O bridge between two hexanuclear units. These ditopic connections generate 46-membered macrocycles (Figure 32, right) that, in turn, lead to 2D waved CPs.<sup>41</sup>



View Article Online  
DOI: 10.1039/C7CE00009J

**Figure 32** – The hexanuclear species **46** (left) and the 46-membered macrocycle generated through bpy and formate bridges (right). In the latter figure H atoms, coordinated and crystallization water molecules, monatomic formate anions and pyrazolate carbon atoms are omitted for clarity.

The reaction of the TTC acetate derivative **50**<sup>55</sup> with bpy yielded results similar to those observed in the case of formate derivative, three bpy containing compounds, **48**, **49** and **22** being indeed obtained, as function of the bpy/Cu<sub>3</sub> reaction ratio.<sup>42</sup> Compound **48**, prepared in MeOH with bpy/Cu<sub>3</sub> = 2, consists of the hexanuclear fragment shown in Figure 33, left. Besides bpy molecules, one acetate ion also connects the TTC units, through a monatomic O bridge, generating condensed 46-membered macrocycles (one of which is shown in Figure 33, right), resulting in a series of parallel, but offset stacked, 2D CPs.

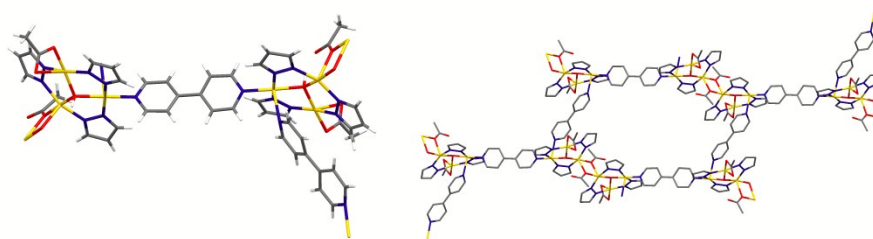


**Figure 33** – The hexanuclear species **48** (left), where crystallization water and MeOH molecules are omitted for clarity. On the right a macrocycle generated through acetate and bpy bridges.

With bpy/Cu<sub>3</sub> = 4, the hexanuclear species **49** (Figure 34) was instead obtained,<sup>42</sup> where two trinuclear fragments are connected by two ditopic bpy molecules, acetate anions behaving as monatomic ligands. Another monatomic bpy is coordinated to each trinuclear unit and further bpy molecules are present in the crystal lattice together with water and methanol.

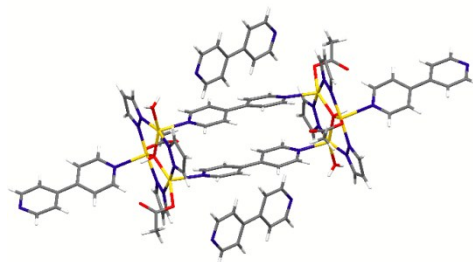


**Figure 34** – The hexanuclear species **49**. Crystallization water and MeOH molecules are omitted for clarity.

A further increase of the bpy/Cu<sub>3</sub> ratio yielded the hexanuclear species **22**<sup>42</sup> which is isomorphous, at rt, with the previously discussed compound **18**.<sup>41</sup> Analogously to **18**, pores of compound **22**, accounting for about 23% solvent accessible void space, partly contain bpy and, also in this case, soaking with suitable solvents leads to the exchange of this molecule. Moreover, a reversible single-crystal-to-single-crystal process, yielding the derivative **23**, takes place on cooling **22** at 100 K. In Figure 35 are shown the structures of both **22** and **23**, evidencing a twist of the structure, passing from rt to 100 K.

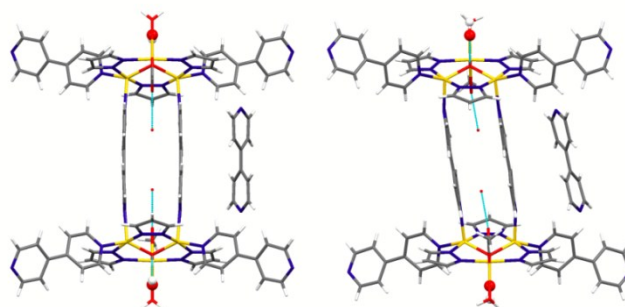


**Figure 35** – Molecular structures of the hexanuclear species **22** collected at rt (left), and **23** collected at 100 K (right). Uncoordinated OH ions are evidenced by ball-and-stick representation.

The reaction of the propanoate TTC specie **53**<sup>7</sup> with bpy yielded the hexanuclear compound **54**<sup>42</sup> characterized by a structure almost superimposable to that of the acetate based derivative **48**, as shown in Figure 36. Also the 2D CP obtained through propanoate and bpy bridges is almost identical to that of **48**.

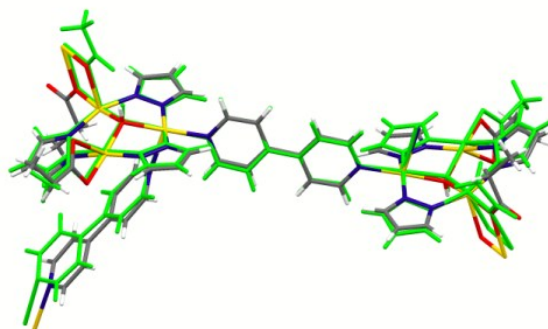


**Figure 36** – Molecular structure of the hexanuclear species **54** superimposed to that of **48** (evidenced by green color). Crystallization molecules have been removed from both structures for clarity.

By reacting both the acrylate TTC derivatives **62** and **63** with bpy in a molar ratio bpy/Cu<sub>3</sub> = 2, a unique compound, **60**, (Figure 37) formed.<sup>42</sup> Due to the ditopic behavior of one acrylate anion and bpy, a series of condensed 30-membered macrocycles generates the 1D tape shown in Figure 37.

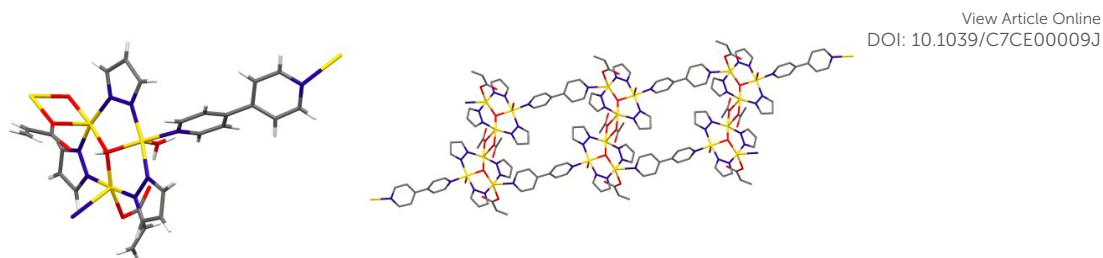


**Figure 37** – The molecular structures of **60** (left) and the 1D tape generated by condensed macrocycles (right), where H atoms have been omitted for clarity.

When compound **62** was treated with a large excess of bpy (bpy/Cu<sub>3</sub> = 8), the TTC species **61** was instead obtained<sup>42</sup>. In this compound (see Figure 38) acrylate anions behave as monotopic ligands, and the formation of a 1D tape is ensured by bpy. Moreover, due to a peculiar competition between coordination and formation of a H-bond, only one bpy molecule acts as a ditopic ligand generating the tape, even though also the second one seems to have an orientation apt to coordinate copper (Figure 38, right).

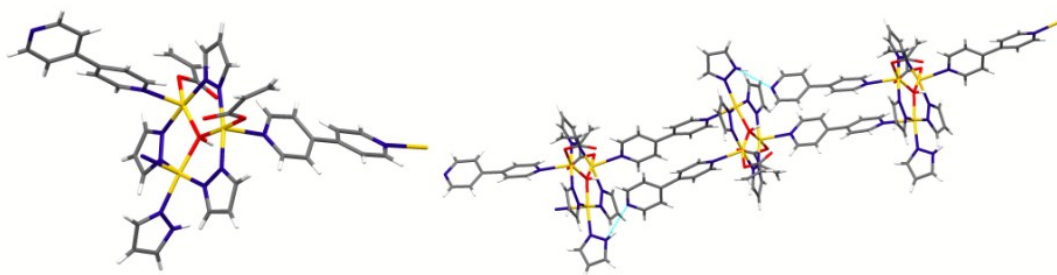
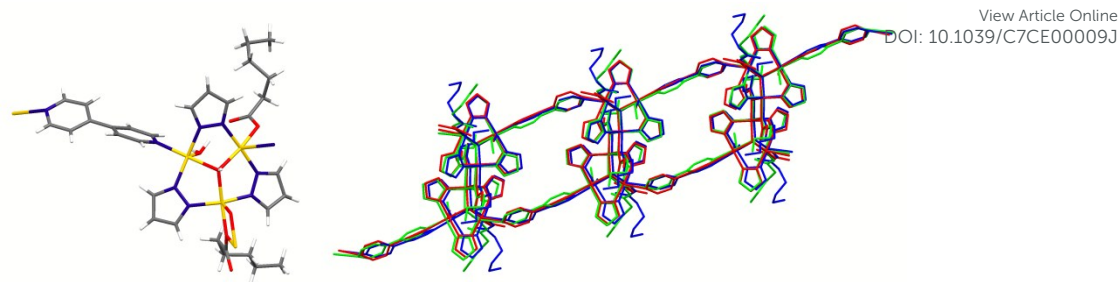


**Figure 38** – Molecular structure of **61** (left) and the 1D tape generated by the ditopic behavior of one bpy molecule (right). Cyan dotted lines indicate the H-bonds competing with pyridyl nitrogen coordination.

The reactivity of TTC derivatives toward bpy, in methanol, was further tested on the butyrate TTC derivative **56**,<sup>54</sup> and also on the not structurally characterized valerate, hexanoate and heptanoate trinuclear species.<sup>9</sup> Butyrate and hexanoate derivatives generated compounds **81** and **82**, respectively,<sup>56</sup> in which, analogously to compound **80**,<sup>41</sup> the capping  $\mu_3$ -OH is substituted by the  $\mu_3$ -OMe fragment. While compound **82** was obtained by using a high bpy/Cu<sub>3</sub> ratio (8:1), when a lower reaction ratio was employed the TTC derivative **58** (Figure 39, left) formed and an analogous TTC structure (**57**) was obtained in the reaction of the valerate trinuclear derivative with bpy. Moreover, also the assemblies of **58** and **57** are almost identical<sup>56</sup> and superimposable to that of the previously discussed acrylate derivative **60**,<sup>42</sup> as sketched in Figure 39.



View Article Online

DOI: 10.1039/C7CE00009J

**Figure 39** – Molecular structure of **58** (left) and partial sketches of superimposed 1D tapes of **58** (blue), **57** (green) and **60** (red) (right), where H atoms have been omitted for clarity.

Finally, the reaction of the not structurally characterized heptanoate trinuclear derivative<sup>9</sup> with bpy yielded the hexanuclear compound **59**,<sup>56</sup> where the ditopic behavior of one carboxylate and bpy generate the 1D CP shown in Figure 40.

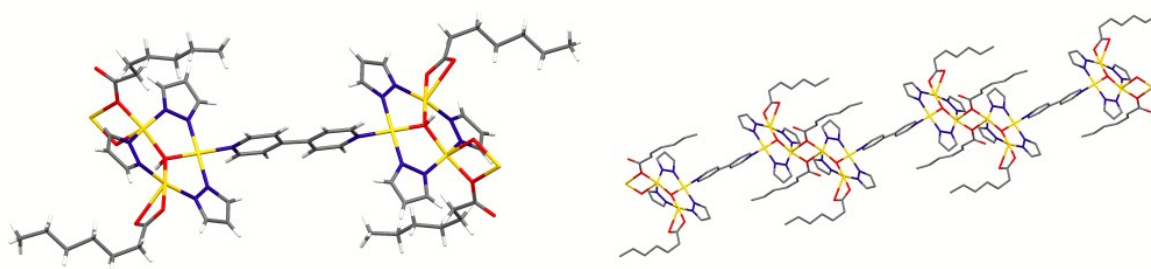


**Figure 40** – Molecular structure of **59** (left) and partial sketch of 1D CP (right), where H atoms have been omitted for clarity.

## Applications and characteristics

From literature it appears that the TTC derivatives are potentially interesting for some useful applications. First of all, the triangular copper(II) array, having a geometry close to the equilateral one, offers the opportunity to study the so called spin-frustration phenomenon.<sup>3,11,12,65</sup> Actually, a large number of reports concerning TTC derivatives evidences the occurrence of magnetic exchange, leading to magnetic moment values close to that corresponding to one unpaired electron, thus indicating a strong antiferromagnetic coupling.<sup>7,9,31,39,41,42,45-47,49,50,52-58,60,61,63</sup> In some cases further coupling between TTC units occurs, likely due to H-bonds or other supramolecular interactions<sup>45,46,52</sup> while, only for compounds **76-78**, a strong ferromagnetic coupling has been reported.<sup>62</sup>

Likely due to intrinsic difficulties to correctly mimic the structural and electronic features of “true” TTC derivatives containing, besides the  $\text{Cu}_3(\mu_3\text{-OH})(\mu\text{-pz})_3$  fragment plus charge balancing anion(s), coordinated water, alcohols, pyrazole or other nitrogen ligands and often displaying strong supramolecular interactions, theoretical calculations on TTC moieties have been performed in few cases. More specifically, theoretical calculations based on the density functional theory have got insights on a TTC derivative electronic structure,<sup>55</sup> allowed an accurate assignment of a TTC UV-Vis



spectrum,<sup>54</sup> indicated a possible mechanism of the H<sup>+</sup> electrophilic attack to a TTC moiety,<sup>39</sup> and let to propose a possible pathway for the formation of the tetranuclear derivative  $[\{\text{Cu}_2(\mu\text{-pz})(\mu\text{-OCH}_2\text{COO})(\text{Hpz})(\text{MeOH})\}_2(\mu\text{-ClCH}_2\text{COO})_2]$ , obtained in the reaction of copper(II) chloroacetate with Hpz.<sup>40</sup> Moreover, theoretical calculations have been also employed to explore the nature of TTCs magnetic exchange.<sup>47,49,50,52,53,63</sup>

TTC derivatives have been tested as catalysts (or catalyst precursors) in some relevant reactions, resulting active in cyclopropanation,<sup>55</sup> photodegradation of organic dyes,<sup>30,62</sup> peroxidative oxidation of cycloalkanes,<sup>7,9,41,57</sup> and styrene oxidation by H<sub>2</sub>O<sub>2</sub>.<sup>60</sup> While in most cases the TTC compounds are dissolved in the reaction media and may be questionable what is the active species, the photodegradation of organic dyes occurs in heterogeneous conditions,<sup>30,62</sup> by using CPs having TTC moieties as SBUs. On the other hand, it should be noted that when TTC derivatives were dissolved in the reaction media in the presence of acid and small quantity of oxidants, the permanence of the trinuclear structure has been confirmed by spectroscopy, suggesting that TTC-derivates could be also the catalytic species.

It is relevant that the TTC units can be employed as SBUs in the building of stable CPs, as evidenced by the isolation of compounds **1** and **71-78**. In this context, and taking into account the displacement of monocarboxylates ions by strong acids, (compounds **2**, **16**, **17**, **27**, **28**, **31**, **32**, **37**, **38**, **42** and **51**), it is reasonably to expected that the reaction of TTCs based on monocarboxylates with suitable bi- or tricarboxylic acids may lead to the formation of polydimensional CPs, possibly characterized by tunable porosity. Moreover, the possibility to react TTC containing compounds with suitable di-, tri- or polytopic nucleophiles, yielded numerous 1-, 2- and 3D CPs (compounds **25**, **40**, **41**, **45**, **46**, **48**, **54**, **57-61**), supramolecular porous derivatives (compounds **18-23**), a hexanuclear derivative **49**, besides an interpenetrated 3D CP (**80**) and two 1D CPs (**81**, **82**) where the  $\mu_3\text{-OH}$  is substituted by the  $\mu_3\text{-OME}$  moiety.

Finally, Wang *et al.*<sup>66</sup> employed the  $[\text{Cu}_3(\mu_3\text{-OH})(\mu\text{-pz})_3(\text{MeCOO})_2(\text{Hpz})]$  derivative **50** as precursor in the solvothermal reaction leading to the formation of a peculiar copper(I) derivative Cu<sub>2</sub>L (L = 3,3',5,5'-tetraethyl-4,4'-bipyrazolate) which self-assembles generating a very stable porous 3D CP useful for selective hydrocarbons sorption in water.

## Conclusions and Perspectives

Neutral and ionic trinuclear triangular Cu<sup>II</sup> arrays based on the  $\text{Cu}_3(\mu_3\text{-OH})(\text{pz})_3$  moiety can be easily prepared by reaction of copper(II) carboxylates with Hpz and water, through a spontaneous self-assembly process when the basicity of the carboxylate or of the anionic counter-ion is adequate to yield sufficient amounts of pz<sup>-</sup> and OH<sup>-</sup> anions or upon addition of an exogenous base or through solvothermal reactions. This reaction is very significant as copper complexes with varying nuclearity are the active

sites of a number of proteins and enzymes and that in the last years several researchers encapsulates for example, copper(II) acetate in zeolites in order to activate O<sub>2</sub> and then to mimic the oxygenase activity of the enzymes.<sup>67</sup> A systematic and detailed study on the reaction between unsubstituted pyrazole and more than 25 different copper(II) carboxylates has been performed, highlighting all specific spectroscopic and structural features of the TTC afforded.<sup>68</sup>

Substantially different structures can be obtained depending on the counter-ion denticity and flexibility, employed solvent, capability of all species to generate supramolecular structures through coordinative and H-bonds or van der Waals interactions, leading in several cases to the formation of 1D, 2D or 3D CPs. Particularly, 3D CPs, in some cases porous, can be easily obtained by using di- or tricarboxylates.

The TTC moiety is very stable, often being resistant to strong acids attacks which displace the original counter-ion(s) maintaining, in a relevant extent, the triangular array. By exploiting this reactivity new CPs and supramolecular networks, characterized by different porosity and solubility can be generated. The TTC fragment is also tolerant to several nucleophiles such as mono-dentate N-donor ligands or multitopic bridging species as 4,4'-bpy, that upon displacement of monodentate ligands can connect each-other single TTC arrays, generating poly-dimensional CPs or supramolecular networks.

The relevant stability of the TTC moieties is likely the key of their possible future uses. Particularly, the possibility to react TTC containing compounds with suitable di-, tri- or polytopic nucleophiles, open the way to employ these derivatives as building blocks according to crystal engineering procedures.

Even though a relatively low number of applications for these TTC arrays have been reported, nevertheless they have been efficiently employed as catalysts or catalysts precursors in some relevant reactions. Finally, TTC derivatives evidence magnetic properties related to the spin-frustration phenomenon, displaying magnetic susceptibility approximately corresponding to one unpaired electron.

## Acknowledgements

The Universities of Padova and Camerino are acknowledged for funds. The authors are indebted to the following colleagues and students that, in the last twelve years contributed to the studies on the fascinating world of TTCs: S. Carlotto, M. Casarin, A. Cingolani, F. Condello, S. Contaldi, C. Corvaja, M. F. C. G. da Silva, C. Di Nicola, D. Falcomer, L. Franco, E. Forlin, F. Garau, M. Gazzano, Y. Yu. Karabach, A. M. Kirillov, A. Lanza, L. M. D. R. S. Martins, N. Masciocchi, S. Massignani, M. Monari, M. M. Natile, F. Nestola, A. J. L. Pombeiro, R. Pettinari, F. Piccinelli, D. Pucci, R. Scatena, P. Tagliatesta, A. Zorzi, F. Zorzi.

## Notes and references

<sup>§</sup> Hereafter, to shortly indicate the Cu<sub>3</sub>(μ<sub>3</sub>-OH)(μ-pz)<sub>3</sub> moiety the acronym TTC (Trinuclear Triangular Copper) will be used.

<sup>§§</sup> Hereafter, the structurally characterized compounds will be indicated by using consecutive bold numbers. In Table A (see below) a complete list of the discussed compounds is reported, accompanied

by the corresponding Identifiers and Compounds Names found in the Structure Navigator of Mercury 3.8 CCDC database. Mercury Article Online  
DOI: 10.1039/C7CE00009J

Table A - List of structurally characterized TTC compounds with corresponding Identifiers and Compounds Names retrieved from Mercury 3.8 CCDC database.

Entry	Identifier	Compound Name <sup>a</sup>	Ref
1	HAWBIS	catena-(( $\mu_6$ -benzene-1,3,5-tricarboxylato)-( $\mu_3$ -hydroxo)-( $\mu_3$ -oxo)-hexakis( $\mu_2$ -pyrazolato)-hexa-copper(ii))	30
2	QUSMIB	( $\mu_3$ -hydroxo)-tris( $\mu_2$ -pyrazolato-N,N')-tris(1H-pyrazole-N <sup>2</sup> )-tri-copper(ii) ( $\mu_3$ -oxo)-tris( $\mu_2$ -pyrazolato-N,N')-tris(1H-pyrazole-N <sup>2</sup> )-tri-copper(ii) tris(trifluoromethanesulfonate)	31
3	KEWRAG	bis(triphenylphosphine)iminium bis( $\mu_3$ -oxo)-tris( $\mu_2$ -3,5-diphenylpyrazolato)-hexakis( $\mu_2$ -pyrazolato)-hexa-copper(ii)	32
4	NESQOS	tetra-n-butylammonium ( $\mu_3$ -oxo)-tris(( $\mu_2$ -pyrazolato-N,N')-(benzoato-O))-tri-copper(ii)	33
5	XOBCEW01	bis(bis(triphenylphosphine)iminium) ( $\mu_3$ -oxo)-tris( $\mu_2$ -pyrazolato-N,N')-trichloro-tri-copper(ii)	34
6	RUYGIB	tetra-n-butylammonium ( $\mu_3$ -hydroxo)-tris( $\mu_2$ -pyrazolato-N,N')-trichloro-tri-copper(ii)	34
7	RUYHEY	triethylammonium ( $\mu_3$ -hydroxo)-tris( $\mu_2$ -pyrazolato-N,N')-pyrazole-trichloro-tri-copper(ii)	34
8	LUDZIV	bis(tetra-n-butylammonium) octakis( $\mu$ -hydroxo)-octadecakis( $\mu$ -pyrazolato)-pentadeca-copper diphosphate bromobenzene nitrobenzene solvate	35
9	LUDZOB	bis(tetra-n-butylammonium) octakis( $\mu$ -hydroxo)-octadecakis( $\mu$ -pyrazolato)-pentadeca-copper diarsenate bromobenzene nitrobenzene solvate	35
10	MAFBOL	bis(tetrabutylammonium) bis(( $\mu_3$ -hydroxo)-( $\mu_2$ -acetato-O,O)-bis(acetato-O)-tris( $\mu_2$ -pyrazol-1,2-diyl)-tri-copper(ii)) hexahydrate	36
11	XOKWUQ	bis(tetra-n-butylammonium) bis( $\mu_3$ -hydroxo)-hexakis( $\mu_2$ -pyrazolato-N,N')-bis( $\mu_2$ -thiocyanato-N,S)-tetrakis(isothiocyanato)-hexa-copper(ii)	37
12	XEMYEV	bis(triethylammonium) bis( $\mu_3$ -hydroxo)-bis( $\mu_2$ -acetato-O)-hexakis( $\mu_2$ -pyrazolyl)-tetrakis(acetato-O)-hexa-copper(ii) benzene solvate	38
13	RUYGEX	bis(triphenylphosphine)iminium ( $\mu_3$ -hydroxo)-tris( $\mu_2$ -pyrazolato-N,N')-trichloro-tri-copper(ii) tetrahydrofuran dichloromethane solvate	34
14	MAFBEB	bis(triphenylphosphino)iminium ( $\mu_3$ -hydroxo)-tris(( $\mu_2$ -pyrazol-1,2-diyl)-(isocyanato))-tri-copper(ii)	36
15	MAFBIF	bis(bis(triphenylphosphino)iminium) bis(( $\mu_3$ -hydroxo)-( $\mu_2$ -acetato-O,O)-aqua-bis(acetato-O)-tris( $\mu_2$ -pyrazol-1,2-diyl)-tri-copper(ii)) dihydrate	36
16	DIBXES	bis( $\mu_3$ -hydroxo)-bis( $\mu_2$ -acetato-O,O)-hexakis( $\mu_2$ -pyrazolato-N,N')-tetrakis(pyrazole-N <sup>2</sup> )-hexa-copper(ii) dichloride dihydrate	39
17	YUYGUW	bis( $\mu_3$ -hydroxo)-hexakis( $\mu_2$ -pyrazolyl)-bis( $\mu_2$ -chloroacetato)-tetrakis(pyrazole)-hexa-copper bis(chloride)	40
18	KEBBUQ	bis( $\mu_3$ -hydroxo)-hexakis( $\mu_2$ -pyrazolato)-bis( $\mu_2$ -4,4'-bipyridine)-diaqua-tetrakis(4,4'-bipyridine)-bis(formato)-hexa-copper(ii) dihydroxide 4,4'-bipyridine	41
19	KEBCAX	bis( $\mu_3$ -hydroxo)-hexakis( $\mu_2$ -pyrazolato)-bis( $\mu_2$ -4,4'-bipyridine)-diaqua-tetrakis(4,4'-bipyridine)-bis(formato)-hexa-copper(ii) dihydroxide benzene solvate	41
20	KEBCIF	bis( $\mu_3$ -hydroxo)-hexakis( $\mu_2$ -pyrazolato)-bis( $\mu_2$ -4,4'-bipyridine)-diaqua-tetrakis(4,4'-bipyridine)-bis(formato)-hexa-copper(ii) dihydroxide hemikis(4,4'-bipyridine) cyclohexane solvate	41
21	KEBCUR	bis( $\mu_3$ -hydroxo)-hexakis( $\mu_2$ -pyrazolato)-bis( $\mu_2$ -4,4'-bipyridine)-diaqua-tetrakis(4,4'-bipyridine)-bis(formato)-hexa-copper(ii) dihydroxide toluene solvate	41
22	RUGLEM	bis( $\mu$ -4,4'-bipyridine)-bis( $\mu$ -hydroxo)-hexakis( $\mu$ -pyrazolato)-bis(acetato)-diaqua-tetrakis(4,4'-bipyridine)-hexa-copper 4,4'-bipyridine dihydroxide dihydrate	42
23	RUGLIQ	bis( $\mu$ -4,4'-bipyridine)-bis( $\mu$ -hydroxo)-hexakis( $\mu$ -pyrazolato)-bis(acetato)-diaqua-tetrakis(4,4'-bipyridine)-hexa-copper 4,4'-bipyridine dihydroxide tetrahydrate	42
24	XOKXAX	( $\mu_3$ -hydroxo)-tris( $\mu_2$ -pyrazolato-N,N')-tris(pyridine-N)-tri-copper(ii) bis(trifluoromethanesulfonate) acetone solvate	37
25	MUZRIJ	catena-[bis( $\mu_3$ -hydroxo)-tris( $\mu_2$ -4,4'-bipyridine-N,N')-hexakis( $\mu_2$ -pyrazolato-N,N')-hexa-copper(ii) tetrakis(trifluoromethanesulfonate) hexahydrate]	43
26	VIMYEX	( $\mu_3$ -hydroxy)-( $\mu_2$ -chloro)-tris( $\mu_2$ -pyrazole)-(aqua)-tris(1H-pyrazole)-tri-copper dicyano(nitro)methanide monohydrate	44
27	BOFLEP	( $\mu_3$ -hydroxy)-tris( $\mu_2$ -pyrazole)-tetrakis(1H-pyrazole)-bis(nitrato)-di-copper monohydrate	45
28	BOZBIB	catena-( $\mu_3$ -nitrato-O,O',O'')-( $\mu_3$ -hydroxo)-1-nitrato-1,2:1,3:2,3-tris( $\mu_2$ -pyrazolato-N,N')-2,3-bis(pyrazole-N <sup>2</sup> )-tri-copper(ii) monohydrate	46
29	MINZIU	( $\mu$ -hydroxo)-tris( $\mu$ -pyrazolato)-( $\mu$ -nitrato)-tris(pyridine)-(nitrato)-tri-copper	47
30	ZOQGOB	bis(( $\mu_3$ -hydroxo)-( $\mu_3$ -nitrato-O,O')-( $\mu_2$ -nitrato-O,O')-tris( $\mu_2$ -pyrazol-1,2-diyl)-tris(pyrazol-	48

		2-yl))-hexa-copper(ii)	View Article Online DOI: 10.1039/C7CE00009J
31	DIBXIW	catena-(bis( $\mu_3$ -chloro)-bis( $\mu_3$ -hydroxo)-hexakis( $\mu_2$ -pyrazolato-N,N')-diaqua-tetrachloro-hexakis(pyrazole-N <sup>2</sup> )-hepta-copper(ii))	39
32	DIBXOC	bis( $\mu_3$ -hydroxo)-bis( $\mu_2$ -chloro)-hexakis( $\mu_2$ -pyrazolato-N,N')-dichloro-hexakis(pyrazole-N <sup>2</sup> )-hexa-copper(ii) monohydrate	39
33	QIMSIQ	( $\mu_3$ -hydroxy)-tris( $\mu_2$ -pyrazole)-bis(1H-pyrazole)-(N,N-dimethylformamide)-dichloro-tri-copper ( $\mu_3$ -hydroxy)-( $\mu_2$ -chloro)-tris( $\mu_2$ -pyrazole)-bis(1H-pyrazole)-chloro-tri-copper N,N-dimethylformamide solvate	49
34	SIJKOL	( $\mu_3$ -hydroxo)-tris( $\mu_2$ -pyrazole-N,N')-( $\mu_2$ -chloro)-chloro-bis(pyridyl)-tri-copper(ii) pyridine solvate	50
35	BOLXEH	catena-(( $\mu_3$ -hydroxo)-bis( $\mu_2$ -bromo)-tris( $\mu_2$ -pyrazolato)-tetrahydrofuran-tri-copper tetrahydrofuran solvate)	51
36	QOPJIP	bis( $\mu_3$ -perchlorato-O,O',O'')-bis( $\mu_3$ -hydroxo)-bis( $\mu_2$ -perchlorato-O,O')-hexakis( $\mu_2$ -pyrazolato-N,N')-hexakis(pyrazole-N)-hexa-copper(ii) ethanol methanol solvate dihydrate	52
37	QUSLOG	bis( $\mu_3$ -hydroxo)-bis( $\mu_3$ -perchlorato-O,O',O'')-bis( $\mu_2$ -perchlorato-O,O')-hexakis( $\mu_2$ -pyrazolato-N,N')-hexakis(pyrazole-N <sup>2</sup> )-hexa-copper(ii)	31
38	QUSMUN	( $\mu_3$ -hydroxo)-( $\mu_3$ -trifluoromethanesulfonato-O,O',O'')-tris( $\mu_2$ -pyrazolato-N,N')-tris(1H-pyrazole-N <sup>2</sup> )-(trifluoromethanesulfonato-O)-tri-copper(ii) monohydrate	31
39	MUZQUU	( $\mu_3$ -hydroxo)-tris( $\mu_2$ -pyrazolato-N,N')-( $\mu_2$ -trifluoromethanesulfonato-O,O')-tripyridine-(trifluoromethanesulfonato-O)-tri-copper(ii) hemihydrate	43
40	MUZRAB	bis( $\mu_3$ -hydroxo)-( $\mu_2$ -4,4'-bipyridine-N,N')-hexakis( $\mu_2$ -pyrazolato-N,N')-tetrapyridine-hexa-copper(ii) tetrakis(trifluoromethanesulfonato)	43
41	MUZREF	catena-[bis( $\mu_3$ -hydroxo)-bis( $\mu_2$ -4,4'-bipyridine-N,N')-hexakis( $\mu_2$ -pyrazolato-N,N')-dipyridine-hexa-copper(ii) tetrakis(trifluoromethanesulfonato) monohydrate]	43
42	QUSLEW	( $\mu_3$ -hydroxo)-tris( $\mu_2$ -pyrazolato-N,N')-( $\mu_2$ -sulfato-O,O')-tris(pyrazole-N <sup>2</sup> )-tri-copper(ii) monohydrate	31
43	MINZOA	octakis( $\mu$ -(4-methylphenyl)phosphonato)-octakis( $\mu$ -hydroxo)-dodecakis( $\mu$ -pyazolato)-diaqua-tetrapyridine-octadeca-copper acetonitrile unknown solvate tetrahydrate	47
44	DOKKAQ	catena-(( $\mu_6$ -sulfato)-bis( $\mu_3$ -hydroxo)-hexakis( $\mu_2$ -pyrazolato-N,N)-bis( $\mu_2$ -nitrato)-hexakis(1H-pyrazole-N)-hexa-copper acetonitrile methanol solvate sesquihydrate)	53
45	KEBBOK	catena-(tetrakis( $\mu_3$ -hydroxo)-dodecakis( $\mu_2$ -pyrazolato)-( $\mu_2$ -4,4'-bipyridine)-tetrakis( $\mu_2$ -formato)-diaqua-tetrakis(formato)-dodeca-copper(ii) decahydrate)	41
46	KEBDEC	catena-(bis( $\mu_3$ -hydroxo)-hexakis( $\mu_2$ -pyrazolato)-( $\mu_2$ -4,4'-bipyridine)-bis( $\mu_2$ -formato)-diaqua-bis(4,4'-bipyridine)-bis(formato)-hexa-copper(ii) dihydrate)	41
47	JAVGAP	catena-(( $\mu_3$ -hydroxo)-( $\mu_2$ -formato)-tris( $\mu_2$ -pyrazole)-formato-bis(pyrazol-2-yl)-tri-copper(ii) monohydrate)	54
48	RUGKUB	catena-[bis( $\mu$ -acetato)-bis( $\mu$ -4,4'-bipyridine)-bis( $\mu$ -hydroxo)-hexakis( $\mu$ -pyrazolato)-bis(acetato)-hexa-copper methanol solvate monohydrate]	42
49	RUGLAI	catena-[bis( $\mu$ -4,4'-bipyridine)-( $\mu$ -hydroxo)-tris( $\mu$ -pyrazolato)-bis(acetato)-aqua-tri-copper 4,4'-bipyridine methanol solvate tetrahydrate]	42
50	LAHYUP	catena-[( $\mu_3$ -acetato)-( $\mu_3$ -hydroxo)-( $\mu_2$ -acetato)-tris( $\mu_2$ -pyrazolyl)-(pyrazole)-tri-copper(ii)]	55
51	QUSMEX	( $\mu_3$ -hydroxo)-tris( $\mu_2$ -pyrazolato-N,N')-( $\mu_2$ -trifluoroacetato-O,O')-bis(1H-pyrazole-N <sup>2</sup> )-(trifluoroacetato-O)-tri-copper(ii)	31
52	JEWWEO	( $\mu_3$ -hydroxo)-tris( $\mu_2$ -pyrazolato)-aqua-bis(propionato)-tri-copper(ii) monohydrate	7
53	JEWWIS	( $\mu_3$ -hydroxo)-tris( $\mu_2$ -pyrazolato)-aqua-bis(propionato)-tri-copper(ii)	7
54	RUGLUC	catena-[bis( $\mu$ -4,4'-bipyridine)-bis( $\mu$ -hydroxo)-bis( $\mu$ -propanoato)-hexakis( $\mu$ -pyrazolato)-bis(propanoato)-hexa-copper dihydrate]	42
55	JAVGET	catena-(( $\mu_3$ -hydroxo)-( $\mu_2$ -propionato-O,O)-( $\mu_2$ -propionato-O,O')-tris( $\mu_2$ -pyrazole)-ethanol-tri-copper(ii))	54
56	JAVGIX	bis(( $\mu_3$ -hydroxo)-( $\mu_2$ -butyrato)-tris( $\mu_2$ -pyrazole)-aqua-butyrato-methanol-tri-copper(ii))	54
57	HUTZED	catena-[( $\mu_3$ -hydroxo)-tris( $\mu_2$ -pyrazolyl)-( $\mu_2$ -4,4'-bipyridine)-( $\mu_2$ -valerato)-(valerato)-methanol-tri-copper]	56
58	HUTZON	catena-[( $\mu_3$ -hydroxo)-( $\mu_2$ -4,4'-bipyridine)-tris( $\mu_2$ -pyrazolyl)-( $\mu_2$ -hexanoato)-(hexanoato)-aqua-tri-copper]	56
59	FUPYOG	catena-[bis( $\mu$ -hydroxo)-bis( $\mu$ -heptanoato)-(4,4'-bipyridine)-hexakis( $\mu$ -pyrazolato)-bis(heptanoato)-hexa-copper]	56
60	RUGMEN	catena-[( $\mu$ -4,4'-bipyridine)-( $\mu$ -hydroxo)-( $\mu$ -acrylato)-tris( $\mu$ -pyrazolato)-(acrylato)-aqua-tri-copper]	42
61	RUGMOX	catena-[( $\mu$ -4,4'-bipyridine)-( $\mu$ -hydroxo)-tris( $\mu$ -pyrazolato)-(acrylato-O)-(acrylato-O,O')-(4,4'-bipyridine)-(1H-pyrazole)-tri-copper dihydrate]	42

62	XUCRET	bis( $\mu_3$ -hydroxo)-bis( $\mu_2$ -acrylato-O,O)-hexakis( $\mu_2$ -pyrazolato-N,N')-bis(acrylato-O,O')-tetra-aqua-bis(pyrazole-N <sup>2</sup> )-hexa-copper(ii)	57
63	XUCRIX	catena-(( $\mu_3$ -hydroxo)-( $\mu_2$ -acrylato-O,O')-( $\mu_2$ -acrylato-O,O)-tris( $\mu_2$ -pyrazolato-N,N')-methanol-tri-copper(ii))	57
64	XUCROD	catena-(( $\mu_3$ -hydroxo)-bis( $\mu_2$ -methacrylato-O,O')-tris( $\mu_2$ -pyrazolato-N,N')-tri-copper(ii))	57
65 <sup>b</sup>	1454767	( $\mu_3$ -hydroxo)-tris( $\mu$ -pyrazolato)-bis(pivalato)-(pyrazole)-bis(pivalic acid)-tri-copper(ii)	58
66 <sup>b</sup>	1454763	catena-(( $\mu_3$ -hydroxo)-bis( $\mu$ -phenylacetato-O,O')-tris( $\mu$ -pyrazolato-N,N')-tri-copper(ii))	58
67 <sup>b</sup>	1454764	catena-(( $\mu_3$ -hydroxo)-( $\mu_3$ -vinylacetato)-( $\mu$ -vinylacetato)-tris( $\mu$ -pyrazolato-N,N')-tri-copper(ii))	58
68 <sup>b</sup>	1454765	bis(( $\mu_3$ -hydroxo)-( $\mu_3$ -phenylpropanoato)-( $\mu$ -phenylpropanoato)-tris( $\mu$ -pyrazolato-N,N')-tri-copper(ii))-bis(( $\mu_3$ -hydroxo)-( $\mu_3$ -phenylpropanoato)-( $\mu$ -phenylpropanoato)-tris( $\mu_2$ -pyrazolato-N,N')-diaqua-tri-copper(ii))	58
69 <sup>b</sup>	1454766	catena-(( $\mu_3$ -hydroxo)-bis( $\mu$ -cyclohexylcarboxylato-O,O')-tris( $\mu$ -pyrazolato-N,N')-tri-copper(ii))	58
70	DEGBAU	bis( $\mu_3$ -hydroxo)-tetrakis( $\mu_2$ -hydroxo)-hexadecakis( $\mu_2$ -pyrazolato)-bis(isocyanato)-dodeca-copper methanol solvate	59
71	TAZWOI	catena-[( $\mu_3$ -fumarato)-( $\mu_3$ -hydroxo)-tris( $\mu_2$ -pyrazolyl)-(1H-pyrazole-N <sup>2</sup> )-tri-copper(ii)]	60
72	TAZWUO	catena-[( $\mu_3$ -2-methylfumarato)-( $\mu_3$ -hydroxo)-tris( $\mu_2$ -pyrazolyl)-(1H-pyrazole-N <sup>2</sup> )-tri-copper(ii)]	60
73	CENJIQ	catena-(( $\mu_3$ -succinato)-( $\mu_3$ -hydroxo)-tris( $\mu_2$ -pyrazolato)-aqua-(methanol)-tri-copper monohydrate unknown solvate)	61
74	CENKAJ	catena-(( $\mu_3$ -succinato)-( $\mu_3$ -hydroxo)-tris( $\mu_2$ -pyrazolato)-triaqua-tri-copper hemihydrate unknown solvate)	61
75	CENKEN	catena-(( $\mu_4$ -succinato)-( $\mu_3$ -hydroxo)-tris( $\mu_2$ -pyrazolato)-tri-copper)	61
76 <sup>c</sup>	QOJZEW01	catena-[( $\mu$ -2-hydroxynaphthalene-1,4-dicarboxylato)-( $\mu$ -hydroxo)-tris( $\mu$ -pyrazolato)-tri-copper N,N-dimethylformamide methanol solvate monohydrate]	62
77 <sup>c</sup>	QOJZIA01	catena-[( $\mu$ -biphenyl-4,4'-dicarboxylato)-( $\mu$ -hydroxo)-tris( $\mu$ -pyrazolato)-diaqua-tri-copper]	62
78 <sup>c</sup>	QOKCOK01	catena-(( $\mu_3$ -oxo)-( $\mu_3$ -pyridine-3,4-dicarboxylato)-tris( $\mu_2$ -pyrazolato)-diaqua-methanol-tri-copper unknown solvate)	62
79	HUXWUU	tris( $\mu$ -3,5-diphenylpyrazolato)-( $\mu$ -fluoro)-bis( $\mu$ -hydroxo)-hexakis( $\mu$ -pyrazolato)-hexa-copper(ii) unknown solvate	63
80	KEBBEA	catena-(( $\mu_3$ -methoxido)-tris( $\mu_2$ -pyrazolato)-( $\mu_2$ -4,4'-bipyridine)-( $\mu_2$ -formato)-(formato)-tri-copper(ii) methanol solvate)	41
81	FUPYIA	catena-[bis( $\mu$ -methoxo)-bis( $\mu$ -butanoato)-hexakis( $\mu$ -pyrazolato)-bis( $\mu$ -4,4'-bipyridine)-bis(butanoato)-hexa-copper]	56
82	HUTZIH	catena-[bis( $\mu_3$ -methoxy)-bis( $\mu_2$ -4,4'-bipyridine)-bis( $\mu_2$ -hexanoato)-hexakis( $\mu_2$ -pyrazolyl)-bis(hexanoato)-hexa-copper]	56

<sup>a</sup> The Compound Names reported in Table A do not respect, in almost all cases, the 2005 IUPAC Recommendations for the Nomenclature of Inorganic Compounds. Nevertheless, we have maintained the Compounds Names retrieved from the Structure Navigator of Mercury 3.8 CCDC database, with the aim to avoid the possibility that, a search on the CCDC database fails if the "correct" compound name is used. <sup>b</sup> For compounds **65-69** reported in ref. 58 the CCDC deposit numbers are indicated. <sup>c</sup> Atomic coordinates of compounds **76-78** (QOJZEW01, QOJZIA01 and QOKCOK01) (ref. 62) can be retrieved from the corresponding QOJZEW, QOJZIA and QOKCOK files, reported in the CCDC database as Personal Communication.

<sup>§§§</sup> If not otherwise stated, in all the figures cyan and red dotted lines indicate H-bonds and hanging H-bonds, respectively.

- 1) G. A. Ardizzoia, S. Cenini, M. Moret and N. Masciocchi, *Inorg. Chem.*, 1991, **30**, 4347.
- 2) G. A. Ardizzoia, M. Angaroni, G. La Monica, C. Cariati, S. Cenini, N. Masciocchi and M. Moret, *Inorg. Chem.*, 1994, **33**, 1458.
- 3) A. P. Cole, D. E. Root, P. Mukherjee, E. I. Solomon and T. D. P. Stack, *Science*, 1996, **273**, 1848.
- 4) V. Mahadevan, R. Gebbink and T. D. P. Stack, *Curr. Opin. Chem. Biol.*, 2000, **4**, 228.
- 5) W. B. Tolman and E. A. Lewis, *Chem. Rev.*, 2004, **104**, 1047.
- 6) A. M. Kirillov, M. N. Kopylovich, M. V. Kirillova, M. Haukka, M. F. C. Guedes da Silva and A. J. L. Pombeiro, *Angew. Chem., Int. Ed.*, 2005, **44**, 4345.

- 7) C. Di Nicola, Y. Yu. Karabach, A. M. Kirillov, M. Monari, L. Pandolfo, C. Pettinari and A. J. L. Pombeiro, *Inorg. Chem.*, 2007, 46, 221. View Article Online  
DOI: 10.1039/C7CE00009J
- 8) R. A. Himes and K. D. Karlin, *Curr. Opin. Chem. Biol.*, 2009, 13, 119.
- 9) C. Di Nicola, F. Garau, Y. Y. Karabach, L. M. D. R. S. Martins, M. Monari, L. Pandolfo, C. Pettinari and A. J. L. Pombeiro, *Eur. J. Inorg. Chem.*, 2009, 666.
- 10) S. Hazra, S. Mukherjee, M. F. C. Guedes da Silva and A. J. L. Pombeiro, *RCS Adv.*, 2014, 4, 48449.
- 11) *Magnetic Molecular materials*; D. Gatteschi, O. Kahn, J. S. Miller, F. Palacio, Eds.; NATO ASI Series 198; Kluwer Academic Publishers: Dordrecht, The Netherlands, 1991.
- 12) S. Ferrer, F. Lloret, I. Bertomeu, G. Alzuet, J. Borrás, S. Garcia-Granda, M. Liu-Gonzalez and J. G. Haasnoot, *Inorg. Chem.*, 2002, 41, 5821.
- 13) J-C. Liu, G-C. Guo, J-S. Huang and X-Z. You, *Inorg. Chem.*, 2003, 42, 235.
- 14) J. Yoon and E. I. Solomon, *Coord. Chem. Rev.*, 2007, 251, 379.
- 15) T. Afrati, C. Dendrinou-Samara, C. Raptopoulou, A. Terzis, V. Tangoulis, A. Tsipis and D. P. Kessissoglou, *Inorg. Chem.*, 2008, 47, 7545.
- 16) W. Ouellette, H. Liu, C. J. O'Connor and J. Zubieta, *Inorg. Chem.*, 2009, 48, 4655.
- 17) K. Darling, W. Ouellette, A. Prosvirin, S. Freund, K. Dunbar and J. Zubieta, *Cryst. Growth Des.*, 2012, 12, 2662.
- 18) S. Ferrer, F. Lloret, E. Pardo, J. Clemente-Juan, M. Liu-Gonzalez and S. Garcia-Granda, *Inorg. Chem.*, 2012, 51, 985.
- 19) A. Escuer, G. Vlahopoulou, F. Lloret and F. A. Mautner, *Eur. J. Inorg. Chem.*, 2014, 83.
- 20) M. Dong, P. Yang, X. Liu, B. Xia, Z. Chen, Y. Ling, L. Weng, Y. Zhou and J. Sun, *Cryst. Growth Des.* 2015, 15, 1526.
- 21) A. Messerschmidt, A. Ressi, R. Ladenstein, R. Huber, M. Bolognesi, G. Gatti, A. Marchesini and A. Finazzi-Agro, *J. Mol. Biol.*, 1989, 206, 513.
- 22) R. Huber, *Angew. Chem., Int. Ed.*, 1989, 28, 848.
- 23) A. Messerschmidt, R. Ladenstein, R. Huber, M. Bolognesi, L. Avigliano, R. Petruzzelli, A. Rossi and A. Finazzi-Agro, *J. Mol. Biol.*, 1992, 224, 179.
- 24) E. I. Solomon, U. M. Sundaram and T. E. Machonkin, *Chem. Rev.*, 1996, 96, 2563.
- 25) W. Kaim and J. Rall., *Angew. Chem., Int. Ed.*, 1996, 35, 43.
- 26) R. H. Holm, P. Kennepohl and E. I. Solomon, *Chem. Rev.*, 1996, 96, 2239.
- 27) S-K. Lee, S. DeBeer George, W. E. Antholine, B. Hedman, K. O. Hodgson and E. I. Solomon, *J. Amer. Chem. Soc.*, 2002, 124, 6180.
- 28) E. I. Solomon, A. J. Augustine and J. Yoon, *Dalton Trans.*, 2008, 3921.
- 29) CCDC researches were carried out at November, 2016. Compounds where also metal different from copper are present have been excluded.
- 30) H. Zhang, Y. Lu, Z-m. Zhang and E-b Wang, *Inorg. Chem. Commun.* 2012, 17, 9.
- 31) C. Di Nicola, F. Garau, M. Gazzano, M. Monari, L. Pandolfo, C. Pettinari and R. Pettinari, *Cryst. Growth Des.*, 2010, 10, 3120.
- 32) G. Mezei, M. Rivera-Carrillo and R. G. Raptis, *Dalton Trans.*, 2007, 37.
- 33) G. Mezei, J. E. McGrady and R. G. Raptis, *Inorg. Chem.*, 2005, 44, 7271.
- 34) P. A. Angaridis, P. Baran, R. Boca, F. Cervantes-Lee, W. Haase, G. Mezei, R. G. Raptis and R. Werner, *Inorg. Chem.*, 2002, 41, 2219.
- 35) G. Mezei, *Chem. Commun.*, 2015, 51, 10341.
- 36) G. Mezei, M. Rivera-Carrillo and R. G. Raptis, *Inorg. Chim. Acta*, 2004, 357, 3721.
- 37) M. Rivera-Carrillo, I. Chakraborty, G. Mezei, R. D. Webster and R. G. Raptis, *Inorg. Chem.*, 2008, 47, 7644.
- 38) M. A. Yakovleva, E. V. Kushan, N. S. Boltacheva, V. I. Filyakova and S. E. Nefedov, *Zh. Neorg. Khim. (Russ.) (Russ. J. Inorg. Chem.)*, 2012, 57, 181.
- 39) M. Casarin, A. Cingolani, C. De Nicola, D. Falcomer, M. Monari, L. Pandolfo and C. Pettinari, *Cryst. Growth Des.*, 2007, 7, 676.
- 40) S. Carlotto, M. Casarin, A. Lanza, F. Nestola, L. Pandolfo, C. Pettinari and R. Scatena, *Cryst. Growth Des.*, 2015, 15, 5910.

- 41) C. Di Nicola, F. Garau, M. Gazzano, M. F. C. G. da Silva, A. Lanza, M. Monari, F. Nestola, L. Pandolfo, C. Pettinari and A. J. L. Pombeiro, *Cryst. Growth Des.*, 2012, 12, 2890. View Article Online  
DOI: 10.1039/C2CE00009J
- 42) C. Di Nicola, F. Garau, M. Gazzano, A. Lanza, M. Monari, F. Nestola, L. Pandolfo and C. Pettinari, *Cryst. Growth Des.*, 2015, 15, 1259.
- 43) M. Rivera-Carrillo, I. Chakraborty and R. G. Raptis, *Cryst. Growth Des.*, 2010, 10, 2606.
- 44) M. R. Razali, A. Urbatsch, G. B. Deacon and S. R. Batten, *Polyhedron*, 2013, 64, 352.
- 45) A. Alsalmeh, M. Ghazzali, R. A. Khan, K. Al-Farhan and J. Reedijk, *Polyhedron*, 2014, 75, 64.
- 46) F. B. Hulsbergen, R. W. M. ten Hoedt, G. C. Verschoor, J. Reedijk and A. L. Spek, *J. Chem. Soc., Dalton Trans.*, 1983, 539.
- 47) J. A. Sheikh, H. S. Jena, A. Adhikary, S. Khatua and S. Konar, *Inorg. Chem.*, 2013, 52, 9717.
- 48) K. Sakai, Y. Yamada, T. Tsubomura, M. Yabuki and M. Yamaguchi, *Inorg. Chem.*, 1996, 35, 542.
- 49) Y. M. Davydenko, S. Demeshko, V. A. Pavlenko, S. Dechert, F. Meyer and I. O. Fritsky, *Z. Anorg. Allg. Chem.*, 2013, 639, 1472.
- 50) M. Angaroni, G. A. Ardizzioia, T. Beringhelli, G. La Monica, D. Gatteschi, N. Masciocchi and M. Moret, *J. Chem. Soc., Dalton Trans.*, 1990, 3305.
- 51) W. A. Wallace, G. J. Nilsen, B. D. Piazza, M. Mourigal, J. Hauser, H. M. Ronnow and K. W. Kramer, *CSD Communication (Private Communication)*, 2014.
- 52) Q-J. Zhou, Y-Z. Liu, R-L. Wang, J-W. Fu, J-Y. Xu and J-S. Lou, *J. Coord. Chem.*, 2009, 62, 311.
- 53) L-L. Zheng, J-D. Leng, S-L. Zheng, Y-C. Zhaxi, W-X. Zhang and M-L. Tong, *CrystEngComm*, 2008, 10, 1467.
- 54) M. Casarin, C. Corvaja, C. Di Nicola, D. Falcomer, L. Franco, M. Monari, L. Pandolfo, C. Pettinari and F. Piccinelli, *Inorg. Chem.*, 2005, 44, 6265.
- 55) M. Casarin, C. Corvaja, C. Di Nicola, D. Falcomer, L. Franco, M. Monari, L. Pandolfo, C. Pettinari, F. Piccinelli and P. Tagliatesta, *Inorg. Chem.*, 2004, 43, 5865.
- 56) F. Condello, F. Garau, A. Lanza, M. Monari, F. Nestola, L. Pandolfo and C. Pettinari, *Cryst. Growth Des.*, 2015, 15, 4854.
- 57) S. Contaldi, C. Di Nicola, F. Garau, Y. Yu. Karabach, L. M. D. R. S. Martins, M. Monari, L. Pandolfo, C. Pettinari and A. J. L. Pombeiro, *Dalton Trans.*, 2009, 4928.
- 58) S. Massignani, R. Scatena, A. Lanza, M. Monari, F. Condello, F. Nestola, C. Pettinari, F. Zorzi and L. Pandolfo *Inorg. Chim. Acta*, 2017, 455P2, 618.
- 59) L. Mathivathanan, M. Rivera-Carrillo and R. G. Raptis, *Inorg. Chim. Acta*, 2012, 391, 201.
- 60) C. Di Nicola, E. Forlin, F. Garau, A. Lanza, M. M. Natile, F. Nestola, L. Pandolfo and C. Pettinari, *J. Organomet. Chem.*, 2012, 714, 74.
- 61) C. Di Nicola, E. Forlin, F. Garau, M. Gazzano, A. Lanza, M. Monari, F. Nestola, L. Pandolfo, C. Pettinari, A. Zorzi and F. Zorzi, *Cryst. Growth Des.*, 2013, 13, 126.
- 62) S. Bala, S. Bhattacharya, A. Goswami, A. Adhikary, S. Konar and R. Mondal, *Cryst. Growth Des.*, 2014, 14, 6391.
- 63) L. Mathivathanan, K. Al-Ameed, K. Lazarou, Z. Trávníček, Y. Sanakis, R. Herchel, J. E. McGrady and R. G. Raptis, *Dalton Trans.*, 2015, 44, 20685.
- 64) M. Eddaoudi, D. B. Moler, H. Li, B. Chen, T. M. Reineke, M. O'Keeffe and O. M. Yaghi, *Acc. Chem. Res.*, 2001, 34, 319.
- 65) O. Kahn, *Phys. Lett.*, 1979, 265, 109.
- 66) J-H. Wang, M. Li and D. Li, *Chem-Eur. J.*, 2014, 20, 12004.
- 67) C. L. Hill, I. A. Weinstock, *Nature*, 1997, 388, 332.
- 68) C. Pettinari, N. Masciocchi, L. Pandolfo, D. Pucci, *Chem.-Eur. J.*, 2010, 16, 1106.

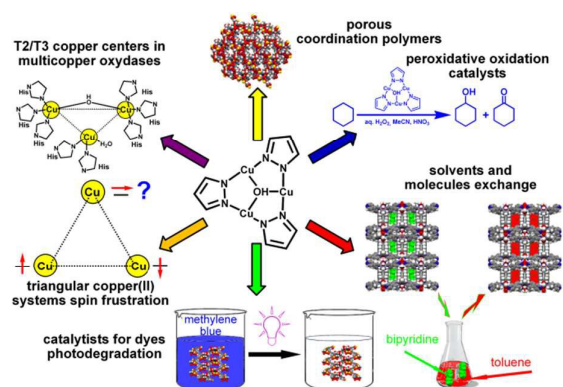
Table of contents for:

## Trinuclear copper(II) pyrazolate compounds: a long story made of serendipitous discoveries and rational design.

by

Luciano Pandolfo and Claudio Pettinari

Graphic



Text

The easy obtaining of the triangular  $\text{Cu}_3(\mu_3\text{-OH})(\mu\text{-pz})_3$  moiety (pz = pyrazolate), its supramolecular self-assemblies, uses and perspectives are reviewed.